

SANDIA REPORT

SAND2008-5983

Unlimited Release

Printed November 2008

Propagating uncertainty through a quadratic response surface model

Vladik Kreinovich, Janos G. Hajagos, W. Troy Tucker, Jan Beck, Lev R. Ginzburg, and Scott Ferson

Prepared by
Sandia National Laboratories
Albuquerque, New Mexico 87185 and Livermore, California 94550

Sandia is a multiprogram laboratory operated by Sandia Corporation,
a Lockheed Martin Company, for the United States Department of Energy's
National Nuclear Security Administration under Contract DE-AC04-94AL85000.

Approved for public release; further dissemination unlimited.



Sandia National Laboratories

Issued by Sandia National Laboratories, operated for the United States Department of Energy by Sandia Corporation.

NOTICE: This report was prepared as an account of work sponsored by an agency of the United States Government. Neither the United States Government, nor any agency thereof, nor any of their employees, nor any of their contractors, subcontractors, or their employees, make any warranty, express or implied, or assume any legal liability or responsibility for the accuracy, completeness, or usefulness of any information, apparatus, product, or process disclosed, or represent that its use would not infringe privately owned rights. Reference herein to any specific commercial product, process, or service by trade name, trademark, manufacturer, or otherwise, does not necessarily constitute or imply its endorsement, recommendation, or favoring by the United States Government, any agency thereof, or any of their contractors or subcontractors. The views and opinions expressed herein do not necessarily state or reflect those of the United States Government, any agency thereof, or any of their contractors.

Printed in the United States of America. This report has been reproduced directly from the best available copy.

Available to DOE and DOE contractors from

U.S. Department of Energy
Office of Scientific and Technical Information
P.O. Box 62
Oak Ridge, TN 37831

Telephone: (865) 576-8401
Facsimile: (865) 576-5728
E-Mail: reports@adonis.osti.gov
Online ordering: <http://www.osti.gov/bridge>

Available to the public from

U.S. Department of Commerce
National Technical Information Service
5285 Port Royal Rd.
Springfield, VA 22161

Telephone: (800) 553-6847
Facsimile: (703) 605-6900
E-Mail: orders@ntis.fedworld.gov
Online order: <http://www.ntis.gov/help/ordermethods.asp?loc=7-4-0#online>



SAND2008-5983
Unlimited Release
Printed November 2008

Propagating uncertainty through a quadratic response surface model

Vladik Kreinovich, Janos G. Hajagos, W. Troy Tucker,
Jan Beck, Lev R. Ginzburg, and Scott Ferson

Applied Biomathematics
100 North Country Road
Setauket, New York 11733 USA

Abstract

This report describes techniques for the propagation of inputs with epistemic uncertainty through a black-box function that can be well characterized by a deterministic quadratic response surface model. The approach uses ellipsoidal representations of uncertain numbers such as intervals and Dempster-Shafer structures over the real line. A particular efficiency that makes calculations comparatively easy arises from the combination of ellipsoidal inputs and a quadratic response surface. The multivariate version of an interval is often thought to be a rectangle or box, but this generalization is not the only one possible. This report explores an alternative generalization based on ellipsoids that facilitates the characterization of inter-variable dependencies. Calculations are much easier than they would be with rectangular intervals because simultaneous diagonalizations can be used both to account for dependencies and to eliminate interaction terms of the quadratic function.

Acknowledgments

This report was developed for Sandia National Laboratories under contract 19094, with project direction by William Oberkampf. We thank Jon Helton and Laura Swiler of Sandia National Laboratories who offered many helpful comments. We also thank Kari Sentz of Los Alamos National Laboratory, Yan Bulgak of the American Museum of Natural History, and Nick Friedenberg of Applied Biomathematics for their unflagging help. The opinions expressed herein are solely those of the authors.

This report will live electronically at <http://www.ramas.com/quadratic.pdf>. Please direct any questions, corrections, or suggestions for improvements to Scott Ferson at scott@ramas.com.

Table of contents

Executive summary	7
Notation	8
1 Introduction	9
2 Approximate quadratic models	11
2.1 Constructing the approximate model	15
3 Standard structures for uncertainty	17
3.1 Intervals	17
3.2 Dempster-Shafer structures on the real line	18
3.3 Interval vectors	19
4 Ellipses and ellipsoids	21
4.1 Describing model inputs	24
4.2 Eliciting the ellipsoid	26
4.3 Simple numerical example	28
5 Quadratic forms	30
5.1 Diagonalizing two quadratic forms	31
6 Finding the range of a quadratic function over an ellipsoid	35
6.1 Algorithm	39
6.2 Simple numerical example (continued)	41
6.3 Intervals of correlation	47
6.4 Nested families of intervals of correlation	50
7 Propagating Dempster-Shafer structures	50
Appendices	53
Appendix 1. Formulas for the ellipsoid from expert information	53
Appendix 2. Formulas to optimize quadratic functions over ellipsoids	57
Glossary	59
References	61

Table of figures

1. Relationship between number of inputs and needed black-box evaluations	13
2. Geometric demonstration of the wrapping effect	21
3. Inner and outer ellipse bounds for an interval vector	23
4. Geometric demonstration of joint diagonalization	33
5. Ellipse of dependency between two intervals	54

Executive summary

The number of uncertain inputs and the computational complexity of some black-box codes can severely constrain our ability to propagate uncertainty through them. This report explores the use of efficient quadratic models for approximating the functions underlying such black-box codes. Multidimensional ellipsoids can characterize uncertainty regarding the inputs to these systems and propagate it through to the output with only minor increases in the computational burden over what is minimally necessary to describe the black-box function with a response surface model. These methods fill a growing need for means to analyze extremely computationally expensive models and legacy codes.

Uncertainty analysis characterizes the uncertainty in model inputs and propagates it through to the model output. Well known methods include sensitivity analysis, Monte Carlo simulation, interval analysis, probability bounds analysis, and Dempster-Shafer theory. Conventional uncertainty propagation methods are either numerical, requiring many repeated evaluations of the model, or they are applied sequentially to the individual binary operations that comprise the function. These methods break down when presented with black-box functions that are very expensive to sample and whose precise functional form is not available for easy inspection.

The methods described in this report make use of a well known result from the theory of quadratic functions (Belman 1960, section 4.12). Under certain conditions, two functions can be simultaneously diagonalized by the same linear transformation of the variables. This transformation can be used to solve the repeated variables problem in the quadratic model and simultaneously account for the dependence matrix among uncertain inputs. This allows uncertainty regarding the precise value of input parameters to be described in the form of intervals that range from the minimum to the maximum value each input could possibly take. Mathematical programming techniques may then be employed to solve the quadratic characterization of the black box for its minimum and maximum values subject to the uncertain interval inputs.

For many expensive black box models, the number of available samples may often be insufficient to estimate a quadratic form for the black-box function or the uncertain inputs using standard fitting algorithms or statistics. This report also presents new algorithms for eliciting information from experts to complete the characterization of these underdetermined systems that take full advantage of the favorable properties exhibited by quadratic functions.

For pedagogical reasons, the presentation includes simple numerical examples involving 2 or 3 input variables. Despite this, all of the ideas are perfectly general, and the method works for an arbitrary n -dimensional problem. Indeed, standard computational tools are available to make the required calculations.

Notation

\underline{X}	the lower bound of the interval X
\tilde{x}	the midpoint of the interval X
\overline{X}	the upper bound of the interval X
Δ_X	the half-width of the interval X
$[a, b]$	an interval with lower bound a and upper bound b
\mathbf{x}	a vector
$\ \mathbf{x}\ $	the norm (Euclidean length) of a vector
\mathbf{X}	a matrix
\mathbf{X}^t	transpose of matrix \mathbf{X}
\mathbf{X}^{-1}	inverse of matrix \mathbf{X}
$\det \mathbf{X}$	determinant of matrix \mathbf{X}
\in	is an element of
\approx	is approximately
$\stackrel{\text{def}}{=}$	is defined to be
\sum	summation
\emptyset	the empty set

1 Introduction

In principle, all measured parameters are uncertain, at least to the precision of the measuring instrument and often much more so. Likewise, theoretically derived parameters are only as certain as the theory upon which they are based, and models themselves are generally incomplete and uncertain. Depending on the parameter and the model, some of these uncertainties may exert a large impact on model results and interpretation. The purpose of uncertainty analysis is to fully characterize the extent and nature of uncertainty in model inputs and propagate it through the model in order to calculate, understand, and make decisions that take into account uncertainty in the output.

Uncertainty can be categorized into two primary types: *variability* and *incertitude*. Variability (also called randomness, aleatory uncertainty, objective uncertainty, or irreducible uncertainty) arises from natural stochasticity, environmental variation across space or through time, and other sources. Incertitude (also called epistemic uncertainty, or subjective uncertainty) arises from incomplete knowledge about the world. Sources of incertitude include measurement uncertainty, small sample sizes, detection limits and data censoring, ignorance about the details of the mechanisms and processes involved, and other imperfections in scientific understanding. Sensitivity analysis, Monte Carlo simulation, Bayesian methods such as Bayes model averaging, interval analysis, and Dempster-Shafer theory are a few of the ways uncertainty can be propagated through mathematical functions and analyzed.

Many methods for uncertainty propagation are applied sequentially to the individual binary operations (the additions, multiplications, etc.) that make up a calculation. Such methods have been called “intrusive” because they require knowledge of the exact nature and sequence of these operations. This knowledge may not always be available. In many applications, for example, an algorithm for computing a function $f(x_1, \dots, x_n)$ of uncertain quantities x_1, \dots, x_n may be written in a language for which a parser is not available, or may exist only as a compiled executable file, or may simply be too complicated for direct use to be practical or even possible.

In such situations, when we have no easy way to analyze the code and decompose it into a sequence of arithmetic operations, the only thing to do is take this program as a *black box*. To propagate uncertainty, one can apply the black-box function to different real-valued inputs and use the results of this sampling to characterize the uncertainty of the output. Such black-box strategies are reviewed by Trejo and Kreinovich (2000).

An even more challenging problem is when sample evaluations of the black-box function are limited to a relative few. This situation is common when, for example, the program takes a long time for a single run. Alternately, even if time itself is not a constraint, the program may require a supercomputer where each run costs a significant amount of money. We shall call a black box *expensive* if, for any reason,

the number of sample evaluations must be a relative few.

When the number of input parameters, x_1, \dots, x_n , is large, the high dimensionality will require many more sample runs of the black box to achieve an accurate characterization of uncertainty in its value given the uncertain inputs. Under these challenges, it is likely there will be fewer pairs of input values mapped to outputs than would be required by traditional black-box approaches. Given the proliferation of complex computer codes that take weeks to run on massive supercomputers, approaches for propagating uncertainty through expensive black boxes with limited sampling need to be developed.

A new but not entirely satisfactory sampling approach for expensive black boxes was recently developed by Trejo and Kreinovich (2000). The method can be applied when the function around the inputs is assumed to be linear as a Taylor series approximation. This assumption is reasonable if the uncertainty around the inputs is relatively small compared to any nonlinearity of the function. The disadvantage of this method for expensive black boxes, besides being a simulation approach, is that the errors have to be relatively small in order for the assumption of linearity to hold. Yet uncertainty analysis is particularly interested in the impact of gross uncertainties on the model.

In this report, we propose a new algorithm for propagating uncertainty through expensive black boxes that allows for inputs with larger uncertainty and more complex associations between the input parameters. The algorithm entails maximizing and minimizing a quadratic response surface model over an ellipsoidal constraint. The quadratic response surface model is an approximating meta-model, or global surrogate model, that describes the expensive black box. First, coefficients for the response surface are estimated by running the black box, f , a set number of times. For large n , the full quadratic response surface may not be estimated because it requires a larger number of model runs than is available. This large number of runs may be infeasible given the cost of evaluating f . To deal with this, we describe a method for estimating a reduced quadratic response surface model when necessary.

A quadratic response model allows the magnitude of the uncertainty to be varied after the black-box model has been run. This property of the response surface can be exploited to propagate both interval and Dempster-Shafer structures through the black box.

In the next section we describe the use of quadratic models to approximate expensive black boxes. Favorable properties of the quadratic are reviewed including the ability to fit realistically complex non-linear relationships and to be estimated with far fewer samples than more general functions.

In Section 3 we review the use of intervals and Dempster-Shafer structures for characterizing input uncertainty and propagating it through to the output of physics-based models. The undesirable properties of these uncertainty characterizations when used in multidimensional interval vectors are reviewed. This motivates the search for a representation of intervals and Dempster-Shafer structures amenable to

multivariate generalization as vectors.

Section 4 nominates ellipsoids as structures capable of characterizing interval input uncertainty, propagating it through to the uncertain value of the response surface model. An algorithm for eliciting input ellipsoids is presented and a numerical example is given. Operations on quadratic forms are reviewed in Section 5 and the procedure for optimizing the quadratic function given uncertain inputs described by ellipsoids is given in Section 6. This minimization and maximization of the response surface model subject to the ellipsoid constraints calculates the range of uncertainty in the black-box function output that is due to uncertainty in the inputs. The final section generalizes many of these results derived assuming interval uncertainty to cases where input uncertainty can be characterized by Dempster-Shafer structures on the real line.

2 Approximate quadratic models

Consider the problem of finding the *range* of possible values of a function $y = f(x_1, \dots, x_n)$ over the set S of all possible parameter vectors $x = (x_1, \dots, x_n)$. The range of y is an interval $[\underline{y}, \bar{y}]$, where \underline{y} is the smallest possible value of $y = f(x_1, \dots, x_n)$ under the constraint that $(x_1, \dots, x_n) \in S$, and \bar{y} is the largest possible value of y under this constraint. Thus, to find the desired range, we must *optimize* the function $f(x_1, \dots, x_n)$ over the set S of possible parameter vectors.

There are many efficient algorithms for optimizing functions under different constraints. Examples of such algorithms are the simplex algorithm, and Metropolis-Hastings algorithms (Metropolis et al. 1953; Hastings 1970). Most of these algorithms are based on an iterative strategy: we start with one or several initial tries \mathbf{x} , and we apply the function f to these tries. Based on the results of this application, we try to predict how the function will behave for other values of the parameter vector \mathbf{x} , and based on this prediction, we produce a new vector \mathbf{x}_{new} at which—we hope—the value of f will be better than for the previous tries. We then apply f to this new vector \mathbf{x}_{new} , and, based on the results of this application, we update the previous prediction of f 's behavior. From this modified prediction, we produce yet another vector \mathbf{x} , etc. These optimization methods require that we apply f to numerous combinations of parameters, i.e., to numerous values of the parameter vector $\mathbf{x} = (x_1, \dots, x_n)$.

For many systems, this can be done, but some systems are so complex that running the model $f(x_1, \dots, x_n)$ even once may require several hours or even days of computation on a supercomputer. For such extremely complex systems, we can, at best, run the model f only a few times.

Because of this limitation, it may be preferable to run an optimization algorithm on an approximation to the original function $f(x_1, \dots, x_n)$ at each step of this algorithm. To do this, we must provide an *approximation* $f_{\text{approx}}(x_1, \dots, x_n)$ to the function $f(x_1, \dots, x_n)$ that this optimization algorithm can use instead of the

original function $f(x_1, \dots, x_n)$.

How can we get an easy-to-compute approximating model, $f_{\text{approx}}(x_1, \dots, x_n)$, that is reasonably close to the original expensive (i.e. very-hard-to-compute) model, $f(x_1, \dots, x_n)$? A common strategy is to fix a family of easy-to-compute approximating models that depends on several coefficients, compute f as many times as we can afford, and then tune the coefficients based on the results.

For expensive black box codes, a low-order approximating model is generally needed because of the limited number of samples that can be practically computed. The following table shows the relationship between model generality and the number of samples required to estimate the model coefficients. n denotes the number of uncertain inputs.

Surface	Samples to parameterize
Linear	$n + 1$
Quadratic	$n(n - 1)/2 + 2n + 1$
Monotonic	$> 2^n$
General	$\gg 2^n$

The minimum number of samples required to specify the approximating model increases dramatically as the generality of the surface increases. It takes two points to specify a line, three a plane, and so forth. Given $n = 6$ variables, for example, determining a linear model requires an absolute minimum of 7 generic samples. Determining a quadratic surface in 6 variables requires 28 samples. The minimum number of samples required to estimate coefficients for a generic monotonic surface is minimally $2^6 = 64$. Moreover, the number of samples needed is also a sharply increasing function of the dimension of the problem, that is, how many inputs, n , there are to the model.

The most widely used easy-to-compute models are *linear* models

$$f_{\text{approx}}(x_1, \dots, x_n) = f_0 + f_1 \cdot x_1 + \dots + f_n \cdot x_n.$$

To uniquely describe a linear model, we must describe the values of $n + 1$ coefficients f_0, f_1, \dots, f_n . To determine the values of these $n + 1$ coefficients, we must know $n + 1$ different values of the function f . Suppose for some practical problem, however, there are $n \approx 50$ variables and we can afford between $N \approx 100$ and $N \approx 200$ calls to the expensive black box model f . Because $N > n + 1$, we can determine more than the $n + 1$ coefficients needed for a linear model. In such a situation, clearly we can go beyond a linear approximation.

After linear, the next natural approximation is quadratic. Because it is unlikely that many black box codes of interest will be strictly linear, it seems reasonable to seek an approach aimed at a compromise between the oversimplicity of a linear model and the unworkable complexity and consequent computational burden of a general model. Quadratic surfaces are the simplest structures that begin to show

complexities such as maxima, minima, and saddle points that arise from functional tradeoffs in a system response. A quadratic approximates an expensive function $f(x_1, \dots, x_n)$ with the *quadratic* expression

$$f_{\text{approx}}(x_1, \dots, x_n) = f_0 + \sum_{i=1}^n f_i \cdot x_i + \sum_{i=1}^n \sum_{j=1}^n f_{i,j} \cdot x_i \cdot x_j. \quad (1)$$

This expression denotes what is sometimes called the *response surface* model. To describe a general quadratic expression, we need to know one constant coefficient f_0 , n linear coefficients f_i , and $n(n+1)/2$ coefficients $f_{i,j} = f_{ji}$. Thus, we must be able to specify a total of $(1/2) \cdot n^2 + (3/2) \cdot n + 1$ coefficients. Figure 1 depicts how this number increases with the number of input variables.

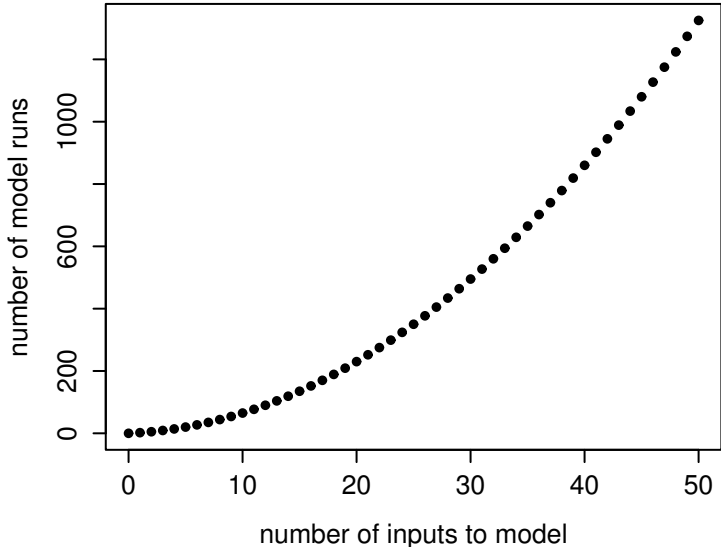


Figure 1: Plot showing the relationship between the number of inputs to the black-box model and the minimum number of times the black box would need to be run to produce a quadratic response surface.

If we can afford the minimum number of runs needed, then the fitting of the coefficients to the results is a straightforward matter using direct calculations (see section 2.1) or statistical regression techniques. When the number of runs mustered is larger than the minimum needed, we can obtain a measure of the unexplained variation in f not accounted for by f_{approx} . Although the differences are likely to be systematic rather than random, this measure is useful as a characterization of how wrong the model is. Visualizing the residuals (observed values of f minus the

values predicted by the fitted model f_{approx}) can be helpful in determining whether the fit is reasonable or not.

On the other hand, we might have fewer than the minimum number of runs needed. For instance, when $n = 50$, we would need

$$\frac{1}{2} \cdot 50^2 + \frac{3}{2} \cdot 50 + 1 = 1,250 + 75 + 1 = 1,326$$

coefficients. If we can only run f at most 100 or 200 times, then we cannot parameterize the full quadratic model. We could, however, use a *restricted* quadratic model, in which we select beforehand a limited number of possible nonzero coefficients $f_{i,j}$. Because we can only use N coefficients, and linear terms require n of them, there are only $N - n$ coefficients left to cover the quadratic terms.

The knowledge of which coefficients $f_{i,j}$ are probably 0 and which may be nonzero can come from the designers or experts who have analyzed the system. How do the corresponding nonzero values affect the system's behavior?

- If $f_{i,i} \neq 0$, this means that the dependence of the desired characteristic y on the corresponding parameter x_i is strongly *nonlinear*.
- If $f_{i,j} \neq 0$, this means that the parameters x_i and x_j are *interdependent* in the sense that the degree to which y depends on x_i is different for different values of x_j .

We can therefore ask experts which parameters and pairs of parameters exhibit such behavior. If there are too many (more than N) such parameters and pairs, we must limit ourselves only to those parameters which are *most* nonlinear and to the pairs which show the *greatest* dependence. To be able to do that, we ask the experts not only to list the parameters that have nonlinear behavior, but also to rank these parameters by the degree of nonlinearity. Section 4.2 describes an algorithm for eliciting the required information.

Once an approximating model is parameterized using available sample data, uncertain input values must be propagated through the approximation. Uncertainty propagation algorithms entail additional computational overhead. The table below contains order-of-magnitude estimates of the computational effort required to both specify the surface via sampling and propagate uncertainty through the resulting model. In this table, the value k represents the computational complexity of propagating the uncertainty. For instance, if uncertainty regarding inputs is characterized using intervals, $k = 2$. For uncertainty characterized using Dempster-Shafer structures, k increases with the number of focal elements used to describe uncertainty regarding the input.

Note that there are certain economies evidenced by the formulas in this table. In particular, as the number of dimensions (n) increases, an approach based on a quadratic model offers a remarkably moderate increase in the computational effort demanded. Projecting uncertainty through the quadratic surface requires effort

Surface	Effort to compute uncertainty
Linear	$nk + n + 1$
Quadratic	$n(n - 1)/2 + 2n + 1 + nk$
Monotonic	$> k2^n$
General	$\gg k2^n$

merely nk higher than the effort needed for sampling alone. This is only an additive increase rather than the multiplicative (k times the sampling effort) increase that would be necessary to propagate uncertain inputs through the more general surfaces.

2.1 Constructing the approximate model

We elicit knowledge from the expert(s) about the model and its input variables in three steps. First, we ask the expert to list all the parameters x_i for which the dependence of the output y on x_i is highly nonlinear. Among all these parameters, we ask the expert to provide a ranking, so that these parameters are listed in the order from the ones that exhibit the largest amount of nonlinear behavior to the ones that exhibit the smallest amount of nonlinearity. Second, we also ask the expert to list all the pairs of parameters (x_i, x_j) which exhibit interdependence, i.e., for which the degree with which the output y depends on x_i is different for different values of x_j . Among all these pairs, we ask the expert to provide a ranking, so that these pairs are listed in the order from the ones that exhibit the largest amount of interdependence to the ones that exhibit the smallest amount interdependence. Third, in addition, we ask the expert to merge the rankings of parameters and pairs into a single ranking. This task may be more difficult and somewhat more subjective.

Then, from this joint ranking, we select $N - n$ top parameters and pairs and develop an approximate model, f_{approx} , (1) in which

- the coefficient $f_{i,i}$ can be different from 0 only if x_i is one of the selected parameters (selected for its high nonlinearity),
- the coefficient $f_{i,j}$ ($i \neq j$) can be different from 0 only if (x_i, x_j) is one of the selected pairs (selected for its high interdependence), and
- all the other coefficients $f_{i,j}$ are equal to 0.

How we determine the values of the nonzero coefficients f_0 , f_i , and $f_{i,j}$ depends on how the samples were selected. There are two possibilities for how sample evaluations are obtained from the black-box model. In the ideal case, we can actually decide which parameter vectors to run through the black-box model. In other situations, we will not have a choice of selecting the parameter vectors. Someone has already selected N different parameter vectors $\mathbf{x}^{(k)} = (x_1^{(k)}, \dots, x_n^{(k)})$, $1 \leq k \leq N$, ran the model for these vectors, and obtain the corresponding N values $y^{(1)}, \dots, y^{(N)}$.

In the unplanned case, we have N linear equations for determining N unknown parameters f_0 , f_i , and $f_{i,j}$:

$$f_0 + \sum_{i=1}^n f_i \cdot x_i^{(k)} + \sum_{i=1}^n \sum_{j=1}^n f_{i,j} \cdot x_i^{(k)} \cdot x_j^{(k)} = y^{(k)}. \quad (2)$$

In this situation, the only way to find these coefficients is to actually solve this system of N linear equations with N unknowns. Solving such a system is feasible for modern computer systems.

In the ideal case, we can select the parameter vectors so as to make the reconstruction of the coefficients much easier, without requiring the solution of any large system of linear equations. Here is the algorithm to do this:

- First, we pick a vector $\mathbf{x}^{(0)} = (x_1^{(0)}, \dots, x_n^{(0)})$ that is inside the zone of possible vectors, and run the model f on this vector. As a result, we get the value $y^{(0)}$.
- For each parameter x_i for which $f_{i,i} = 0$ (i.e., for which there is no nonlinear dependence on x_i), we select a deviation h that keeps us within the zone of possible parameter vectors, forming an input vector

$$\mathbf{x}^{(i)} = (x_1^{(0)}, \dots, x_{i-1}^{(0)}, x_i^{(0)} + h, x_{i+1}^{(0)}, \dots, x_n^{(0)}), \quad (3)$$

and use the model to compute the corresponding value $y^{(i)} = f(\mathbf{x}^{(i)})$. Since $f_{i,i} = 0$, from (2), we conclude that $y^{(i)} - y^{(0)} = f_i \cdot h$, hence f_i can be computed as

$$f_i = \frac{y^{(i)} - y^{(0)}}{h}.$$

The choice of h is arbitrary so long as $x_i^{(0)} + h$ remains within the interval $[\underline{x}_i, \bar{x}_i]$.

- For each parameter x_i with $f_{i,i} \neq 0$, to find the values f_i and $f_{i,i}$, we form the vector (3) and the vector

$$\mathbf{x}^{(-i)} = (x_1^{(0)}, \dots, x_{i-1}^{(0)}, x_i^{(0)} - h, x_{i+1}^{(0)}, x_n^{(0)}).$$

We then use the model f to compute the corresponding values $y^{(i)} = f(\mathbf{x}^{(i)})$ and $y^{(-i)} = f(\mathbf{x}^{(-i)})$. Because $y^{(i)} - y^{(-i)} = 2f_i \cdot h$, we can compute

$$f_i = \frac{y^{(i)} - y^{(-i)}}{2h}.$$

Similarly, because $y^{(i)} + y^{(-i)} - 2y^{(0)} = 2f_{i,i} \cdot h^2$, we can also compute

$$f_{i,i} = \frac{y^{(i)} + y^{(-i)} - 2y^{(0)}}{2h^2}.$$

- Finally, for every interdependent pair (i, j) , to determine $f_{i,j}$, we form a vector

$$\mathbf{x}^{(ij)} = (x_1^{(0)}, \dots, x_{i-1}^{(0)}, x_i^{(0)} + h, x_{i+1}^{(0)}, \dots, x_{j-1}^{(0)}, x_j^{(0)} + h, x_{j+1}^{(0)}, \dots, x_n^{(0)}).$$

Because $y^{(ij)} - y^{(0)} = f_i \cdot h + f_j \cdot h + 2f_{i,j} \cdot h^2$, with the already determined f_i and f_j , we can compute

$$f_{i,j} = \frac{y^{(ij)} - f_i \cdot h - f_j \cdot h}{2h^2}.$$

Caveat. We note that the approach of using the highest degree model compatible with the available number of samples is only reasonable for deterministic models that are fairly well behaved. The approach may not be tenable if there is noise in the output, or the black-box function is overly complicated.

In the rest of this document, we will assume that we already know the coefficients of the quadratic approximation (2).

3 Standard structures for uncertainty

3.1 Intervals

Intervals are a natural way to express uncertainty about the value of a number. An interval is a constraint on the value that a number can take. An interval is defined on the real-line as $\underline{X} \leq x \leq \bar{X}$, where \underline{X} and \bar{X} are known respectively as the infimum and supremum of x . The standard way to write an interval is as a pair of bounds in square brackets, for example $[2.5, 3.5]$. These bounds imply that the value the number can take is equal to or between 2.5 and 3.5.

Intervals can be used in arithmetic calculations. Any binary operation \circ defined on real numbers can be extended to intervals as

$$X \circ Y = \{x \circ y : x \in X, y \in Y\}.$$

Moore (1966) found these formulations devolve to simple rules by which two intervals X and Y can be added, subtracted, multiplied, or divided:

$$\begin{aligned} X + Y &= [\underline{X} + \underline{Y}, \bar{X} + \bar{Y}], \\ X - Y &= [\bar{X} - \underline{Y}, \underline{X} - \bar{Y}], \\ X \times Y &= [\min(\underline{X}\underline{Y}, \bar{X}\bar{Y}, \underline{X}\bar{Y}, \bar{X}\underline{Y}), \max(\underline{X}\underline{Y}, \bar{X}\bar{Y}, \underline{X}\bar{Y}, \bar{X}\underline{Y})], \\ X / Y &= X \times \left[\frac{1}{\bar{Y}}, \frac{1}{\underline{Y}} \right] \text{ given that } 0 \notin Y. \end{aligned}$$

Unary functions and transformations of real numbers are likewise defined by extending the definition to intervals. For instance, the operator for squaring an interval is

$$X^2 = \{x^2 : x \in X\} = \begin{cases} \text{if } \underline{X} > 0 \text{ then } [\underline{X}^2, \bar{X}^2] \\ \text{if } \bar{X} < 0 \text{ then } [\bar{X}^2, \underline{X}^2] \\ \text{if } 0 \in X \text{ then } [0, \max(\underline{X}^2, \bar{X}^2)]. \end{cases}$$

By replacing the standard real arithmetic operations in a mathematical expression with these interval operations we can propagate intervals through the expression.

Example. If we wanted to calculate bounds on the gravitational force exerted by the moon on the earth we would replace the real number operators with interval operators in Newton's universal equation for gravity $F_g = G \frac{m_1 m_2}{r^2}$, where F_g is the force of gravity, m_1 and m_2 are masses of two bodies, G is the universal gravitational constant, and r is the distance between the two bodies. Bounds on G have been calculated to be $[6.672, 6.673] \times 10^{-11} \text{ m}^3 \text{ kg}^{-1} \text{ s}^2$. Bounds on the mass and distance can be inferred from the reported precision in standard sources. The mass of the earth is $[5.98, 5.99] \times 10^{24} \text{ kg}$ and the mass of the moon is $[7.34, 7.35] \times 10^{22} \text{ kg}$. The distance between the centers of the earth and moon is $[3.84, 3.85] \times 10^8 \text{ m}$. We get bounds on the gravitational force exerted by the moon on the earth to be

$$\begin{aligned} F_g &= [6.672, 6.673] \times 10^{-11} \text{ m}^3 \text{ kg}^{-1} \text{ s}^2 \frac{([5.98, 5.99] \times 10^{24} \text{ kg})([7.34, 7.35] \times 10^{22} \text{ kg})}{([3.84, 3.85] \times 10^8 \text{ m})^2} \\ &= [1.97, 2.03] \times 10^{20} \text{ N}. \end{aligned}$$

3.2 Dempster-Shafer structures on the real line

An interval provides no information on where the value is within its bounds. Such questions of location are usually answered by probability theory. Probability theory provides a rich set of tools to deal with uncertainty but at the cost of additional assumptions. For black boxes we may not know the exact distribution of the inputs to the model but we can usually say more about the value than just its interval range. We need a structure that allows us to say more than an interval but not as much as an exact probability distribution about the likelihood a value can take. One option is to put weights of evidence on a collection of intervals. Such structures can be built using the Dempster-Shafer theory of evidence (Dempster 1967; Shafer 1976; 1984; 1986; Klir and Yuan 1995; Sentz and Ferson 2002; Ferson et al. 2003).

A Dempster-Shafer structure is defined on a frame of discernment Ω , which can be, in particular, the real line. Associated with every subset of Ω is a weight of evidence given by a function $m : 2^\Omega \rightarrow [0, 1]$ such that

- $\sum m(A_i) = 1$, and
- $m(\emptyset) = 0$.

A focal element is defined as $A \subseteq \Omega$ for which $m(A) > 0$. For simplicity, we will consider only finite Dempster-Shafer structures for which there are finitely many focal elements A_i , where $i \in \{1, 2, \dots, j\}$. We'll also assume that the focal elements are closed intervals, rather than more complicated sets. Implementation on a computer of such a Dempster-Shafer structure would thus require storage for $3j$ floating-point numbers, one for each mass and two for the corresponding interval.

Dempster-Shafer theory has similarities to both interval analysis and probability theory, and it is a generalization of both. The interval model of uncertainty can be viewed as a special case of a Dempster-Shafer structure with only one element $A_1 \subseteq \Omega = \mathbb{R}$ and $m(A_1) = 1$. A Dempster-Shafer structure on the real line is similar to a discrete probability distribution except that the locations at which the mass resides are *sets* of real values, rather than precise points. These sets associated with nonzero mass are called focal elements. The correspondence of probability masses associated with the focal elements is called the basic probability assignment. This is analogous to the probability mass function for an ordinary discrete probability distribution. Unlike a discrete probability distribution on the real line, where the mass is concentrated at distinct points, the focal elements of a Dempster-Shafer structure may overlap one another, and this is the fundamental difference that distinguishes Dempster-Shafer theory from traditional probability theory.

Yager (1986) defined arithmetic operations between Dempster-Shafer structures that generalize the notions of interval arithmetic as well as convolution between distribution functions. Finite Dempster-Shafer structures on the real line whose focal elements are intervals are especially easy to use in practical calculations.

A Dempster-Shafer structure can capture a wide range of ignorance about the underlying probability that a value can take. A weakness of Dempster-Shafer theory is that it can be difficult to interpret and communicate what the structure means. For a simple Dempster-Shafer structure of two or three focal elements the interpretation is fairly straightforward and can easily be communicated verbally and graphically. However, if the structure has 10 or more elements and some of the elements overlap, the graphical display is more complicated.

3.3 Interval vectors

To handle complex black-box problems in which there are a large number of variables as inputs to the model, a multivariate generalization of the concept of an interval is needed. An interval vector of dimension n is $\mathbf{x} = (x_1, x_2, \dots, x_n)$, where x_i is an interval. For $n = 2$ an interval vector defines a rectangle on the real plane and for $n = 3$ an interval vector defines a box in three-dimensional space. An interval vector is a constraint on the value that a vector can take. Algebraic operators for interval vectors, like intervals, can be defined (Neumaier 1990).

The following example illustrates why, in some cases, interval vectors are inappropriate structures for computing with uncertainty in more than one dimension. Consider the case of a rigid rotation. To perform a rigid rotation of a vector we need to employ multiplication of a vector by a matrix. For $n = 2$, this is

$$\begin{pmatrix} a & b \\ c & d \end{pmatrix} \begin{pmatrix} x_1 \\ x_2 \end{pmatrix} = \begin{pmatrix} a \times x_1 + b \times x_2 \\ c \times x_1 + d \times x_2 \end{pmatrix}.$$

Multiplying a vector by a rotation matrix

$$\mathbf{R} = \begin{pmatrix} \cos \theta & -\sin \theta \\ \sin \theta & \cos \theta \end{pmatrix}.$$

will rotate the vector by θ radians. For example, to rotate the vector $\mathbf{x}^t = (2, 3)$ by π radians (180°) around the origin, we would compute

$$\begin{pmatrix} \cos \pi & -\sin \pi \\ \sin \pi & \cos \pi \end{pmatrix} \begin{pmatrix} 2 \\ 3 \end{pmatrix} = \begin{pmatrix} -1 & 0 \\ 0 & -1 \end{pmatrix} \begin{pmatrix} 2 \\ 3 \end{pmatrix} = \begin{pmatrix} -2 \\ -3 \end{pmatrix}.$$

Let us try something similar for the interval vector $\mathbf{u}^t = ([-1, 1], [-1, 1])$. Suppose we wish to rotate the square defined by the interval vector \mathbf{u} by $\pi/4$ radians (45°):

$$\begin{pmatrix} \cos \frac{\pi}{4} & -\sin \frac{\pi}{4} \\ \sin \frac{\pi}{4} & \cos \frac{\pi}{4} \end{pmatrix} \begin{pmatrix} [-1, 1] \\ [-1, 1] \end{pmatrix} = \begin{pmatrix} \frac{1}{\sqrt{2}} & -\frac{1}{\sqrt{2}} \\ \frac{1}{\sqrt{2}} & \frac{1}{\sqrt{2}} \end{pmatrix} \begin{pmatrix} [-1, 1] \\ [-1, 1] \end{pmatrix} = \begin{pmatrix} [-\sqrt{2}, \sqrt{2}] \\ [-\sqrt{2}, \sqrt{2}] \end{pmatrix} = \mathbf{u}_1.$$

Now we wish to rotate the above answer \mathbf{u}_1 by an additional $\pi/4$ radians. Doing the same calculation as above but substituting \mathbf{u}_1 for \mathbf{u} we get $\mathbf{u}_2^t = ([-2, 2], [-2, 2])$. Rotating the initial interval vector \mathbf{u} by $\pi/2$ radians we get

$$\begin{pmatrix} \cos \frac{\pi}{2} & -\sin \frac{\pi}{2} \\ \sin \frac{\pi}{2} & \cos \frac{\pi}{2} \end{pmatrix} \begin{pmatrix} [-1, 1] \\ [-1, 1] \end{pmatrix} = \begin{pmatrix} 0 & -1 \\ 1 & 0 \end{pmatrix} \begin{pmatrix} [-1, 1] \\ [-1, 1] \end{pmatrix} = \begin{pmatrix} [-1, 1] \\ [-1, 1] \end{pmatrix}.$$

Why do we get two different answers dependent on whether we rotate the interval vector \mathbf{u} once by $\pi/2$ radians or twice by $\pi/4$ radians? Figure 2 shows why the two sequential rotations blow up the bounds on the answer. The vector $\mathbf{u}_1^t = ([-\sqrt{2}, \sqrt{2}], [-\sqrt{2}, \sqrt{2}])$ is not the exact solution set but rather the interval hull solution. The interval hull solution is the interval vector with the smallest width which encloses the solution. It is possible that the interval hull solution contains elements which do not satisfy the constraints. The actual solution set for the rotated vector is enclosed by line segments with the following coordinates $\{(-\sqrt{2}, 0), (0, \sqrt{2}), (\sqrt{2}, 0), (0, \sqrt{2})\}$. So when we do the second rotation of $\pi/4$ radians, we are not rotating the exact solution set but the interval hull. In the second rotation we are getting the interval hull of the rotated interval hull, hence the inflation of the interval vector's width by a factor of 2. Moore (1966) calls this type of inflation the “wrapping effect”. Certain rotations, like $\pi/4$ radians, for interval vectors are not affine transformations. An affine transformation maps parallel lines to parallel lines. What we need is a structure like interval vectors which allows for affine transformations over a larger range of rotations. One possible candidate is the ellipsoid, a multivariate generalization of the ellipse. Before we can explore such use of ellipsoids we need to define what a quadratic form is.

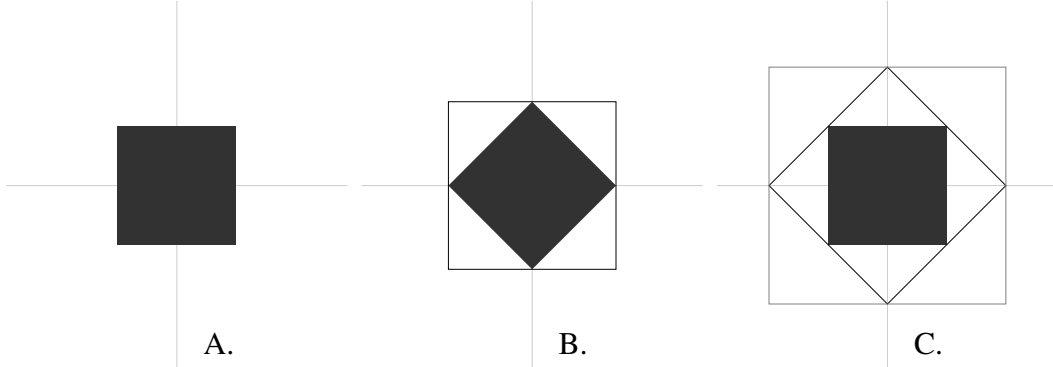


Figure 2: Geometric demonstration of the wrapping effect. Graph A shows the original interval vector $\mathbf{u}^t = ([-1, 1], [-1, 1])$. Graph B shows the vector rotated $\pi/4$ radians and \mathbf{u}_1 , the interval hull solution. Graph C shows the original interval vector rotated a total of $\pi/2$ radians, the rotated interval hull of graph B, and \mathbf{u}_2 the interval hull of the rotated interval hull.

4 Ellipses and ellipsoids

On the real line, an interval is a natural way to represent epistemic uncertainty about a value. In higher-dimensional Euclidean space, there are multiple ways to constrain the value that a vector can take. We could express the constraints as interval vectors, but doing so would expose us to the wrapping effect discussed in section 3.3. We could instead express constraints on the value of \mathbf{x} as $\|\mathbf{x} - \mathbf{x}_0\| \leq C$, where \mathbf{x}_0 is the coordinate of the center of a sphere, and $\|\mathbf{x}\|$ denotes the Euclidean length of the vector. This is a natural way to constrain a value that a vector can take and the constraint has some nice properties, like invariance under rotation around \mathbf{x}_0 . The problem is that the uncertainty in each dimension has to be of equal magnitude. This is unrealistic for parameter inputs to real physical models because there will be a mix of different units where numeric values could be different by orders of magnitude. We need an easy way to specify constraints that allows tighter bounds on the value a vector can take.

A generalization of a sphere that can have different breadths in different dimensions would be an ellipsoid. It turns out that ellipsoids have several advantages that recommend their use in expressing uncertainty (Neumaier 1993; Kreinovich et al. 1998).

The ellipsoid is a multivariate generalization of the ellipse. The ellipse, a conic section, has a major and minor axis. Along the major axis are two foci. Rather than having a single radius like a circle an ellipse has two radii, r_1 and r_2 , one radius originating from the first focus, and the other originating from the second. Their lengths are constrained by the following relation $r_1 + r_2 = 2C$, for some constant C . By varying the location of the foci along the major axis an ellipse can be scaled

along each of the axes. This property will allow an ellipse and its multivariate generalization the ellipsoid to effectively constrain the value a vector can take. An ellipse has a centered form

$$\frac{1}{a^2}x^2 + \frac{1}{b^2}y^2 = 1.$$

Note that this format has no interaction term cxy . The point $\mathbf{a} = (a, 0)$ is the maximal value the ellipse reaches along the x -axis. The point $\mathbf{b} = (0, b)$ has the same property along the y -axis.

An ellipsoid can be *inscribed* within the multivariate rectangle or box if the corners of that box, which represent extremes in multiple variables, are impossible. This ellipsoid projects to each axis as the same univariate interval that described it. Otherwise, the ellipsoid can *circumscribe* the rectangle or box and, even though it will be slightly larger than the box, it will still have favorable properties under rigid rotations needed to account for dependencies. We will call the former the ‘inner ellipse’ and the latter the ‘outer ellipse’.

Given an interval vector $\mathbf{p} = ([5, 10], [1, 3])$, the inner ellipse can be constructed by first computing the half-widths for each element of the vector. For the interval X , the half-width is computed as $\Delta_x = (\bar{X} - \underline{X})/2$. For \mathbf{p} , we have $\Delta_x = (10 - 5)/2 = 5/2$ and $\Delta_y = (3 - 1)/2 = 1$. Let $\alpha = 1/a^2$ and $\beta = 1/b^2$. Then $\alpha = 1/(1^2) = 1$ and $\beta = 1/(5/2)^2 = 4/25$. The constraint, based on \mathbf{p} , is

$$(1)x^2 + (4/25)y^2 = \mathbf{x}^t \begin{pmatrix} 1 & 0 \\ 0 & 4/25 \end{pmatrix} \mathbf{x} \leq 1,$$

with $x = x_0 - (\underline{X} + \bar{X})/2 = (x_0 - 15/2)$ and $y = y_0 - (\underline{Y} + \bar{Y})/2 = (y_0 - 2)$. The formula for the inner ellipse is thus

$$\frac{4}{25}(x - \frac{15}{2})^2 + \frac{1}{1}(y - 2)^2 \leq 1.$$

Figure 3 illustrates how the inner ellipse is inscribed within the interval box. Note that the inner ellipse does not include all possible values of the interval vector. In fact, less than 80% of the values in the box are enclosed by the ellipse. The values that are excluded are those that are simultaneously extreme in multiple dimensions. For instance, the ellipse does not enclose the vector $(x = 5, y = 3)$. This feature of the inner ellipse may make it more attractive as a multivariate model of epistemic uncertainty if such simultaneous extremity is highly unrealistic.

The outer ellipse or elliptical hull should just completely enclose the interval vector \mathbf{p} . The formula for computing the minimal outer ellipse for \mathbf{p} is slightly more complicated than the formula for the inner ellipse. The squared distance from (x_0, y_0) to any of the vertices of the interval vector is $r^2 = \Delta_x^2 + \Delta_y^2$. For the ellipse to intersect the vertices the following equality will hold at a vertex:

$$\alpha\Delta_x^2 + \beta\Delta_y^2 = 1.$$

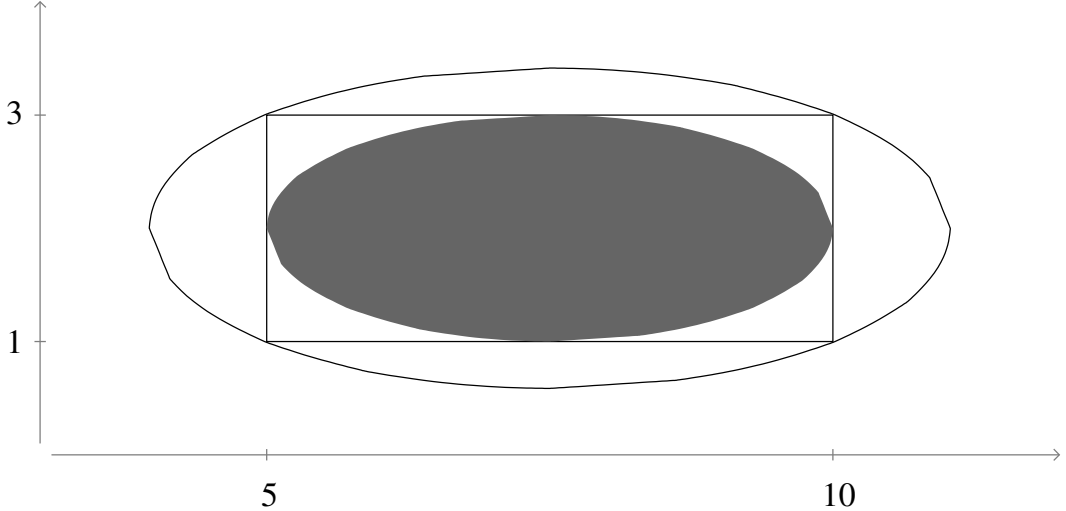


Figure 3: Inner (filled gray) and outer ellipse bounds for the interval vector $\mathbf{p} = ([5, 10], [1, 3])$.

Solving in terms of α and noting that $\Delta_x^2 = r^2 - \Delta_y^2$, we obtain

$$\alpha = \frac{1 - \beta \Delta_y^2}{\Delta_x^2}. \quad (4)$$

The simplest outer bound to compute for \mathbf{p} would be a circle having a center at (x_0, y_0) with a radius $r = \sqrt{(5/2)^2 + 1^2} = \sqrt{29}/4$. Note that by construction this circle intersects each vertex of the interval vector but that it is not an optimal bound on \mathbf{p} . It constrains \mathbf{p} well along the x -axis but not as well along the y -axis. One option to make the fit better is to increase β while recomputing α using equation (4). A more rigorous approach is to find the minimal-area ellipse that encloses the interval vector.

The area of an ellipse is $A = ab\pi$. In terms of α and β , the area is

$$A = \pi \frac{1}{\sqrt{\alpha}} \frac{1}{\sqrt{\beta}}.$$

Substituting for α and with some algebraic manipulations, the area can be written in terms of β , Δ_x , and Δ_y as

$$A = \pi \sqrt{\frac{\Delta_x^2}{(1 - \beta \Delta_y^2)\beta}}.$$

The partial derivative with respect to β is

$$\frac{\partial A}{\partial \beta} = \frac{-\pi \Delta_x (1 - 2\beta \Delta_y^2)}{2(\beta - \beta^2 \Delta_y^2)}.$$

Setting this to zero and solving for β , we find the minimal area for an ellipse occurs when $\beta = 1/2\Delta_y^2$. For the interval vector \mathbf{p} , $\beta = 1/2$. Knowing the value for β , we can compute the value α . The minimal area ellipse enclosing \mathbf{p} is

$$(2/25)x^2 + (1/2)y^2 = \mathbf{x}^t \begin{pmatrix} 2/25 & 0 \\ 0 & 1/2 \end{pmatrix} \mathbf{x} \leq 1.$$

with $x = x_0 - (\underline{X} + \bar{X})/2 = (x_0 - 15/2)$ and $y = y_0 - (\underline{Y} + \bar{Y})/2 = (y_0 - 2)$. Figure 3 also shows how the outer ellipse circumscribes the interval box.

There are some disadvantages to ellipsoids as higher-dimensional structures for representing and propagating uncertainty. Unlike interval vectors, ellipsoids are not closed under set-based operators for addition and subtraction. The Minkowski sum of two ellipsoids is not an ellipsoid.

4.1 Describing model inputs

The first step in uncertainty propagation is to describe the set S of all possible parameter vectors $\mathbf{x} = (x_1, \dots, x_n)$. For many complex systems, this information has to come from experts. For each of the parameters x_i , the experts must provide us with the range of the values of this parameter, i.e., with the interval $[\underline{x}_i, \bar{x}_i]$ of possible values of x_i . Once we know these intervals, we can then guarantee that the possible values of x are inside the box

$$[\underline{x}_1, \bar{x}_1] \times \dots \times [\underline{x}_n, \bar{x}_n]. \quad (5)$$

This does not, however, mean that all the vectors \mathbf{x} within this box are indeed possible. In some cases, there is a correlation or relation of some kind between the parameters x_i . For example, positive correlation between x_1 and x_2 means that, in general, larger values of x_1 correspond to larger values of x_2 , and vice versa. In this case, it is highly unlikely that the parameter x_1 attains its largest possible value \bar{x}_1 , and at the same time the positively related parameter x_2 attains its smallest possible value \underline{x}_2 .

Even when there is no correlation between the two parameters, i.e., if these parameters are, in this sense, independent of each other, not all pairs (x_1, x_2) may be possible. It may be possible that the parameter x_1 attains its extreme value \bar{x}_1 , and it may be possible that the parameter x_2 attains its extreme value \bar{x}_2 , yet it may be reasonable to believe that both extreme situations cannot occur at the same time.

In both the cases of correlation and independence, the set S of possible parameter vectors is a proper subset of the box (5). How can we describe such a subset? Clusters formed by real data points can be circumscribed. The boundary delimits the region where points occur (the cluster) from the region where they don't occur (beyond the cluster). We can describe this boundary by an equation $b(x_1, \dots, x_n) =$

C for some smooth function $b(x_1, \dots, x_n)$ and for some constant C . As a result, the set S itself can be described either by the inequality

$$b(x_1, \dots, x_n) \leq C. \quad (6)$$

An arbitrary smooth function can be approximated by a polynomial, so, instead of the general set (6), we can consider the approximating set

$$a(x_1, \dots, x_n) \leq C, \quad (7)$$

where $a(x_1, \dots, x_n)$ is a polynomial that approximates the function $b(x_1, \dots, x_n)$. As we have already mentioned, the simplest possible polynomials are linear polynomials $a(x_1, \dots, x_n) = a_0 + a_1 \cdot x_1 + \dots + a_n \cdot x_n$. However, for a linear function $a(x_1, \dots, x_n)$, the set of all the vectors \mathbf{x} for which $a(x) \leq C$ is a half-space, i.e., a set that is not bounded in many directions, while we want a set S that is inside the box – and hence, bounded in all directions. Thus, if we restrict ourselves to only linear terms, we do not get a good approximation to the set (6).

To get a reasonable characterization of a bounded set, we must consider at least quadratic polynomial approximating functions $a(x_1, \dots, x_n)$. In particular, for the simplest nonlinear polynomials – quadratic polynomials – the approximating set (7) takes the following form:

$$a(x_1, \dots, x_n) = a_0 + \sum_{i=1}^n a_i \cdot x_i + \sum_{i=1}^n \sum_{j=1}^n a_{i,j} \cdot x_i \cdot x_j \leq C. \quad (8)$$

In principle, an even better description of the actual set (6) would use third-, fourth-, and higher-order polynomials, but describing higher-order approximations would require even more coefficients to be elicited and the resulting structures would therefore be much harder to characterize and manipulate.

For a quadratic function $a(x_1, \dots, x_n)$, the bounded set of all the values of x for which the inequality (8) holds is an *ellipsoid*. It should be understood that ellipsoids have been widely used for the efficient description of uncertainty. For instance, there have been many applications with an interval-analysis perspective in control theory (e.g., Belfonte and Bona 1985; Chernousko 1988; 1994; Filippov 1992; Finkelstein et al. 1996; Fogel and Huang 1982; Schweppe 1968; 1973; Soltanov 1990; Utyubaev 1990). Ellipsoids naturally arise in probabilistic descriptions of uncertainty as well, and this is perhaps the source of most of their popularity. For example, if variability is described by a multidimensional normal distribution, then the confidence set (all the values for which the probability density exceeds a certain threshold) is an ellipsoid. It has been shown experimentally in many practical situations that ellipsoids work better than other families of sets (Chernousko 1988; 1994; Neumaier 1993). Moreover, it has been proven theoretically that ellipsoids indeed form the best family for such purposes under certain reasonable conditions (Finkelstein et al. 1996; Li et al. 2002).

Replacing a rectangular box with a smaller ellipsoid set S makes the range smaller and perhaps more realistic. It also makes this range much easier to compute with. Calculating the range of a quadratic function $f(x_1, \dots, x_n)$ over a rectangular box of intervals is an NP-hard problem (Kreinovich et al. 1998; Vavasis 1991). In contrast, finding the range of a quadratic function over an ellipsoid is a computationally tractable problem (Kreinovich et al. 1998; Trejo and Kreinovich 2001; Vavasis 1991). The following sections will show in detail how this range can be computed.

4.2 Eliciting the ellipsoid

We cannot even use the full quadratic model because we cannot ask experts thousands of questions and expect meaningful answers to all of them. Instead, we have to use a restricted quadratic model, in which we select beforehand a limited number of possible nonzero coefficients $a_{i,j}$.

Let us assume that we can only ask E questions to an expert. In this case, we can only have E nonzero coefficients $a_{i,j}$. We can therefore ask experts which pairs of parameters are correlated. If there are too many (more than E) such pairs, we must limit ourselves only to those pairs which are most correlated (positively or negatively). To be able to do that, we ask the experts not only to list the correlated pairs, but also to rank these pairs by the degree of correlation, so that the expert will be able to select E most correlated pairs.

Once we select E pairs, what can we ask? When the ellipsoid is a confidence set of a general distribution, we can ask about the values of the correlation (in the usual statistical sense) between the variables x_i and x_j . However, in general, an ellipsoid is just a set of possible values of x , with no specific probabilistic meaning, so there is no well-defined statistical correlation, and it would not be reasonable ask an expert about its value.

We can always ask about the correlation in the general sense. As we described it, dependence between x_i and x_j means that the range of possible values of x_i changes depending on the value of x_j . A strong positive correlation means that, when x_j grows, the possible values x_i also become larger, and the values of x_i are the *largest* when x_j attains its largest possible value \bar{x}_j . Similarly, a strong negative correlation means that, when x_j grows, the possible values x_i become smaller, and the values of x_i are the *smallest* when x_j attains its largest possible value \bar{x}_j . To gauge the degree of dependence defined this way between x_i and x_j , we should ask an expert not only to give us the ranges of possible values $[\underline{x}_i, \bar{x}_i]$ and $[\underline{x}_j, \bar{x}_j]$ for the parameters x_i and x_j , but also to describe what values x_i are possible when x_j attains its largest possible value \bar{x}_j . If these values x_i are closer to \bar{x}_i , this means that we have a positive correlation correlation between x_i and x_j . If these value x_i are closer to \underline{x}_i , this means that we have a negative correlation between x_i and x_j .

How we can transform this easy-to-elicit information into the precise description of the ellipsoid (8)? To answer this question, let us first simplify the general formula (8). We start with a very simple step. If we divide both sides of the inequality (8)

by the constant C , we get a slightly simpler description of the general ellipsoid, with one fewer coefficient,

$$a(x_1, \dots, x_n) = a_0 + \sum_{i=1}^n a_i \cdot x_i + \sum_{i=1}^n \sum_{j=1}^n a_{i,j} \cdot x_i \cdot x_j \leq 1. \quad (9)$$

The next simplification step is based on the geometric fact that every ellipsoid has a center $\tilde{x} = (\tilde{x}_1, \dots, \tilde{x}_n)$, and that when we use a coordinate system with the origin at this center, i.e., if we use the differences $\Delta x_i \stackrel{\text{def}}{=} x_i - \tilde{x}_i$ instead of the original values of x_i , the equation for an ellipsoid takes the simplified form

$$a(x_1, \dots, x_n) \stackrel{\text{def}}{=} \sum_{i=1}^n \sum_{j=1}^n a_{i,j} \cdot (x_i - \tilde{x}_i) \cdot (x_j - \tilde{x}_j) \leq 1. \quad (10)$$

In Appendix 1, we describe how we can transform the above easy-to-elicit information into the precise description of the ellipsoid (10). Thus, we arrive at the following algorithm:

- First, we ask the expert(s) to provide, for each parameter x_i , the range $[\underline{x}_i, \bar{x}_i]$ of possible values of x_i .
- Based on these values, we compute the midpoints $\tilde{x}_i = (\underline{x}_i + \bar{x}_i)/2$ and the half-width $\Delta_i = (\bar{x}_i - \underline{x}_i)/2$ of the corresponding intervals.
- Then, we ask the expert to list all the pairs (x_i, x_j) of correlated parameters. Among all these pairs, we ask the expert to provide a ranking, so that the expert will be able to list E most correlated pairs.
- For each possibly correlated pair (x_i, x_j) , we ask the expert: what is the most reasonable value of x_i when $x_j = \bar{x}_j$? We denote the corresponding value by $x_{i,j}$, and compute $\Delta x_{i,j} \stackrel{\text{def}}{=} x_{i,j} - \tilde{x}_i$.
- For all other (i.e., non-correlated) pairs $i \neq j$, we define $\Delta x_{i,j} \stackrel{\text{def}}{=} 0$, and we also take $\Delta x_{j,i} \stackrel{\text{def}}{=} \Delta_j$.
- Based on the known values $x_{i,j}$, \tilde{x}_i , and Δ_i , we compute the components of the symmetric matrix \mathbf{Z} with the components $z_{k,j} \stackrel{\text{def}}{=} \Delta x_{k,j} \cdot \Delta_j$.
- Finally, we invert the matrix \mathbf{Z} . The elements $a_{i,j}$ of the inverse matrix $A = \mathbf{Z}^{-1}$ are exactly the coefficients that describe the ellipsoid (8).

In principle, to invert the matrix, we can use any matrix inversion algorithm (Golub and Loan 1996). However, since our objective is not just to describe the set S of possible values of the parameter vector, but rather to find the range of the quadratic response function $f(x_1, \dots, x_n)$ over the set S , we will see that a special inversion algorithm is the most appropriate here: an algorithm based on finding the eigenvalues and eigenvectors of the matrix \mathbf{Z} .

4.3 Simple numerical example

To illustrate the eliciting algorithm, let us consider the simple example when $n = 2$ and the ellipsoid is the ellipse

$$x_1^2 - x_1 \cdot x_2 + x_2^2 \leq 1. \quad (11)$$

This ellipsoid corresponds to the case when $a_0 = a_1 = a_2 = 0$, and the matrix $\mathbf{A} = (a_{i,j})$ has the following form:

$$\mathbf{A} = \begin{pmatrix} 1 & -1/2 \\ -1/2 & 1 \end{pmatrix}$$

In order to illustrate how our algorithm will reconstruct this ellipsoid, let us first derive the corresponding values of \underline{x}_i and $x_{i,j}$, and then show how the above algorithm reconstructs the ellipsoid.

For the ellipsoid (11), what are the smallest and largest values of x_1 ? For the value x_1 to be possible, it must be possible to have x_2 for which the inequality (11) holds, i.e., for which

$$x_2^2 - x_1 \cdot x_2 + (x_1^2 - 1 + \Delta) = 0 \quad (12)$$

for some $\Delta \leq 0$. The quadratic equation (12) has a solution if and only if its discriminant is non-negative, i.e., if and only if $x_1^2 - 4 \cdot (x_1^2 - 1 + \Delta) \geq 0$. This inequality is, in its turn, equivalent to $4 - 3 \cdot x_1^2 \geq -4 \cdot \Delta$.

Because $\Delta \leq 0$, we infer that if x_1 is possible, then $4 - 3 \cdot x_1^2 \geq 0$. Vice versa, if $4 - 3 \cdot x_1^2 \geq 0$, then we can satisfy the above inequality by taking $\Delta = 0$. Thus, the value x_1 is possible if and only if $4 - 3 \cdot x_1^2 \geq 0$, i.e., if and only if $x_1^2 \leq \frac{4}{3}$.

Thus, the interval of possible values of x_1 is the interval between $-\sqrt{\frac{4}{3}}$ and $+\sqrt{\frac{4}{3}}$, so $\underline{x}_1 = -\frac{2}{\sqrt{3}}$ and $\bar{x}_1 = \frac{2}{\sqrt{3}}$.

Because the formula (11) does not change if we swap x_1 and x_2 , we get exactly the same bounds for x_2 , so $\underline{x}_2 = -\frac{2}{\sqrt{3}}$ and $\bar{x}_2 = \frac{2}{\sqrt{3}}$.

To complete our preliminary analysis, let us find the value $x_{1,2}$, i.e., the value x_1 that is possible when $x_2 = \bar{x}_2$. Substituting $x_2 = \frac{2}{\sqrt{3}}$ into the inequality (11), we get the inequality

$$x_1^2 - \frac{2}{\sqrt{3}} \cdot x_1 + \frac{4}{3} \leq 1,$$

or, equivalently,

$$x_1^2 - \frac{2}{\sqrt{3}} \cdot x_1 + \frac{1}{3} \leq 0.$$

The left-hand side of this inequality is a perfect square, so the inequality implies

$$\left(x_1 - \frac{1}{\sqrt{3}}\right)^2 \leq 0.$$

The square of a real number is always non-negative, so the only case when it is smaller than or equal to 0 is when it actually is equal to 0, i.e., when $x_1 = \frac{1}{\sqrt{3}}$.

Therefore $x_{1,2} = \frac{1}{\sqrt{3}}$.

Let us recount the results of our analysis thus far. We have

$$\underline{x}_1 = -\frac{2}{\sqrt{3}}; \quad \bar{x}_1 = \frac{2}{\sqrt{3}}; \quad \underline{x}_2 = -\frac{2}{\sqrt{3}}; \quad \bar{x}_2 = \frac{2}{\sqrt{3}}; \quad x_{1,2} = \frac{1}{\sqrt{3}}.$$

This is the input to our algorithm.

According to the algorithm, we first compute the midpoints \tilde{x}_i and the half-widths Δ_i of the range intervals. The resulting values are

$$\tilde{x}_1 = \tilde{x}_2 = 0; \quad \Delta_1 = \Delta_2 = \frac{2}{\sqrt{3}}.$$

Next, we compute the values $\Delta x_{i,j}$. The only possibly correlated pair is the pairs (x_1, x_2) , so we compute

$$\Delta x_{1,2} = x_{1,2} - \tilde{x}_1 = \frac{1}{\sqrt{3}} - 0 = \frac{1}{\sqrt{3}}.$$

In accordance with our algorithm, we also set

$$\Delta x_{1,1} = \Delta_1 = \frac{2}{\sqrt{3}}; \quad \Delta x_{2,2} = \Delta_2 = \frac{2}{\sqrt{3}}.$$

We can now compute the components $z_{i,j}$ of the symmetric matrix \mathbf{Z} consisting of

$$\begin{aligned} z_{1,1} &= \Delta x_{1,1} \cdot \Delta_1 = \frac{2}{\sqrt{3}} \cdot \frac{2}{\sqrt{3}} = \frac{4}{3}; \\ z_{2,2} &= \Delta x_{2,2} \cdot \Delta_2 = \frac{2}{\sqrt{3}} \cdot \frac{2}{\sqrt{3}} = \frac{4}{3}; \\ z_{1,2} &= z_{2,1} = \Delta x_{1,2} \cdot \Delta_2 = \frac{1}{\sqrt{3}} \cdot \frac{2}{\sqrt{3}} = \frac{2}{3}. \end{aligned}$$

Thus,

$$\mathbf{Z} = \begin{pmatrix} 4/3 & 2/3 \\ 2/3 & 4/3 \end{pmatrix}.$$

Multiplying \mathbf{Z} by \mathbf{A} , we can see that

$$\begin{pmatrix} 4/3 & 2/3 \\ 2/3 & 4/3 \end{pmatrix} \cdot \begin{pmatrix} 1 & -1/2 \\ -1/2 & 1 \end{pmatrix} = \begin{pmatrix} 1 & 0 \\ 0 & 1 \end{pmatrix},$$

i.e., the inverse matrix to \mathbf{Z} indeed coincides with the original matrix \mathbf{A} describing the ellipse.

5 Quadratic forms

In this section, we introduce quadratic forms and describe some of their properties. We will use these mathematical objects in section 6 to propagate uncertainty. A quadratic form is a quadratic expression, that is, a polynomial of degree 2, that is homogeneous. A quadratic expression is homogeneous if it contains only quadratic terms and no linear or constant terms. An example of such an expression is $x^2 + 3xy + 4y^2$. The quadratic expression $x^2 + 3x + y^2$, on the other hand, is not homogeneous because it contains the linear term $3x$. A three-variable (x, y, z) homogeneous quadratic expression with coefficients $a_{i,j}$

$$a_{1,1}x^2 + a_{2,2}y^2 + a_{3,3}z^2 + a_{1,2}xy + a_{1,3}xz + a_{2,3}yz,$$

can be written

$$(x, y, z)\mathbf{A} \begin{pmatrix} x \\ y \\ z \end{pmatrix} \text{ where } \mathbf{A} = \begin{pmatrix} a_{1,1} & \frac{1}{2}a_{1,2} & \frac{1}{2}a_{1,3} \\ \frac{1}{2}a_{1,2} & a_{2,2} & \frac{1}{2}a_{2,3} \\ \frac{1}{2}a_{1,3} & \frac{1}{2}a_{2,3} & a_{3,3} \end{pmatrix}.$$

For example, the expression $4x^2 + 4y^2 + 4z^2 + 4xy + 4xz + 4yz$ can be expressed in terms of the symmetric matrix for the coefficients

$$\mathbf{A} = \begin{pmatrix} 4 & 2 & 2 \\ 2 & 4 & 2 \\ 2 & 2 & 4 \end{pmatrix}.$$

When a quadratic form has been written in matrix form it can be evaluated as $\mathbf{x}^t \mathbf{A} \mathbf{x}$. For instance, we can evaluate the quadratic expression at $\mathbf{x}^t = (x = -4, y = 2, z = 3)$.

$$(-4, 2, 3) \begin{pmatrix} 4 & 2 & 2 \\ 2 & 4 & 2 \\ 2 & 2 & 4 \end{pmatrix} \begin{pmatrix} -4 \\ 2 \\ 3 \end{pmatrix} = 60.$$

An advantage of placing the coefficients of a quadratic form into a matrix is that the tools of matrix algebra can be used. The matrix \mathbf{A} can be diagonalized, that is, we can find a new vector basis for (x, y, z) that allows \mathbf{A} to be rewritten in terms of products of the diagonal elements of a new matrix. In the new coordinates, the original quadratic form will be expressed in terms of the sum of pure squares. The process of diagonalization involves computing the eigenvalues and eigenvectors of the square matrix.

For the matrix \mathbf{A} , we find three eigenvectors $\mathbf{e}^{(1)} = (-1, 1, 0)$, $\mathbf{e}^{(2)} = (-1, 0, 1)$, $\mathbf{e}^{(3)} = (1, 1, 1)$ and their corresponding eigenvalues $\lambda_1 = 2$, $\lambda_2 = 2$, $\lambda_3 = 8$. These eigenvectors do not form an orthonormal basis. To form an orthonormal basis the eigenvectors need to be mutually perpendicular with each vector having unit length.

We can form an orthonormal basis by applying the Gram-Schmidt orthogonalization process to the eigenvectors. The computed orthonormal basis is a set of row vectors

$$\left\{ \frac{1}{\sqrt{2}}(-1, 1, 0), \frac{1}{\sqrt{6}}(1, 1, -2), \frac{1}{\sqrt{3}}(1, 1, 1) \right\}.$$

Using computer algorithms such orthonormal sets can be computed directly during the diagonalization process (Golub and Loan 1996).

The orthonormal basis defines columns of a new matrix \mathbf{P} . We can transform the coordinates of $\mathbf{x} \rightarrow \mathbf{x}' = \mathbf{P}^t \mathbf{x}$ and use the diagonalization \mathbf{D} formed by the eigenvalues of \mathbf{A} to evaluate the polynomial $\lambda_1(x')^2 + \lambda_2(y')^2 + \lambda_3(z')^2$. In terms of matrices the calculation is:

$$(\mathbf{P}^t \mathbf{x})^t \mathbf{D} (\mathbf{P}^t \mathbf{x}) = 60,$$

where $\mathbf{P} = \begin{pmatrix} \frac{-1}{\sqrt{2}} & \frac{1}{\sqrt{6}} & \frac{1}{\sqrt{3}} \\ \frac{1}{\sqrt{2}} & \frac{1}{\sqrt{6}} & \frac{1}{\sqrt{3}} \\ 0 & \frac{-2}{\sqrt{6}} & \frac{1}{\sqrt{3}} \end{pmatrix}$ and $\mathbf{D} = \begin{pmatrix} 2 & 0 & 0 \\ 0 & 2 & 0 \\ 0 & 0 & 8 \end{pmatrix}.$

Evaluating the transformed quadratic form we get the same answer as when we evaluated the original quadratic form.

The above example is for a three variable quadratic form. However, the matrix approach generalizes to any multivariate quadratic form. For an arbitrary dimension, a quadratic expression $\sum_{i=1}^{i \leq k} \sum_{j=1}^{j \leq k} a_{i,j} x_i x_j$ can be written as a matrix \mathbf{B} where $a_{i,j} = b_{i,j}$ for $i = j$, otherwise $b_{i,j} = b_{j,i} = (1/2)a_{i,j}$.

5.1 Diagonalizing two quadratic forms

This section describes a numerical example of simultaneously diagonalizing two quadratic forms. The ability to do such diagonalizations is the key to optimizing a quadratic function over an ellipsoid while accounting for the dependencies between the variables. Thus, it is also the key to propagating uncertainty through quadratic response surface models of black box codes.

The particular example used in this section is low-dimensional, and it omits linear terms so the calculation is simple enough to follow and check easily, but it illustrates the central idea explored in this report. This idea, of diagonalizing two quadratic forms with the same transformation, relies on an algebraic trick that works when one of the forms is positive definite. An ellipsoid is a level curve of a positive definite quadratic form. The second quadratic form is arbitrary and can be definite, semidefinite, or indefinite.

For the numerical example, we wish to jointly diagonalize the following two quadratic forms:

$$\frac{3}{4}x^2 + \frac{3}{4}y^2 - \frac{1}{2}xy = \mathbf{x}^t \begin{pmatrix} 3/4 & -1/4 \\ -1/4 & 3/4 \end{pmatrix} \mathbf{x} \leq 1, \quad (13)$$

$$f(x, y) = \frac{1}{\sqrt{2}}x^2 - \frac{1}{\sqrt{2}}y^2 + \sqrt{2}xy = \mathbf{x}^t \begin{pmatrix} \frac{1}{\sqrt{2}} & \frac{1}{\sqrt{2}} \\ \frac{1}{\sqrt{2}} & -\frac{1}{\sqrt{2}} \end{pmatrix} \mathbf{x}. \quad (14)$$

Inequality (13) represents an ellipse, and expression (14) is the formula of a saddle-shaped quadratic function. The former is depicted on the top, left graph of Figure 4. Level curves of the saddle are also shown on the top, right of Figure 4.

The various transformations applied to both of these objects are also depicted in the figure. We start by diagonalizing form (13), which yields the matrix $B_{(1)}$ composed of column vectors of eigenvectors and diagonalized matrix $D_{(1)}$,

$$\mathbf{B}_{(1)} = \begin{pmatrix} \frac{1}{\sqrt{2}} & -\frac{1}{\sqrt{2}} \\ \frac{1}{\sqrt{2}} & \frac{1}{\sqrt{2}} \end{pmatrix} \text{ and } \mathbf{D}_{(1)} = \begin{pmatrix} 1 & 0 \\ 0 & 1/2 \end{pmatrix}.$$

In this case the eigenvectors $\{(\frac{1}{\sqrt{2}}, \frac{1}{\sqrt{2}}), (-\frac{1}{\sqrt{2}}, \frac{1}{\sqrt{2}})\}$ form an orthonormal basis $\beta_{(1)}$. We can now rewrite (14) in terms of $\beta_{(1)}$ by using $\mathbf{B}_{(1)}$. Define \mathbf{L} to be a change-of-basis matrix. A change-of-basis transformation for \mathbf{A} is $\mathbf{L}^{-1}\mathbf{A}\mathbf{L}$. An orthonormal matrix is a change of basis matrix. Noting that $\mathbf{B}_{(1)}^{-1} = \mathbf{B}_{(1)}^t$,

$$\mathbf{B}_{(1)}^t \begin{pmatrix} \frac{1}{\sqrt{2}} & -\frac{1}{\sqrt{2}} \\ \frac{1}{\sqrt{2}} & \frac{1}{\sqrt{2}} \end{pmatrix} \mathbf{B}_{(1)} = \begin{pmatrix} \frac{1}{\sqrt{2}} & -\frac{1}{\sqrt{2}} \\ -\frac{1}{\sqrt{2}} & -\frac{1}{\sqrt{2}} \end{pmatrix}$$

In geometric terms the change of basis transformation is a rotation of $-\pi/4$ radians around the origin. At this point, we have two quadratic forms in terms of new coordinates \mathbf{x}' :

$$(x')^2 + \frac{1}{2}(y')^2 = (\mathbf{x}')^t \begin{pmatrix} 1 & 0 \\ 0 & 1/2 \end{pmatrix} \mathbf{x}' \leq 1, \quad (15)$$

$$f(x', y') = \frac{1}{\sqrt{2}}(x')^2 - \frac{1}{\sqrt{2}}(y')^2 - \sqrt{2}x'y' = (\mathbf{x}')^t \begin{pmatrix} \frac{1}{\sqrt{2}} & \frac{1}{\sqrt{2}} \\ \frac{1}{\sqrt{2}} & -\frac{1}{\sqrt{2}} \end{pmatrix} \mathbf{x}'. \quad (16)$$

The next step is a linear transformation to scale (15) to the unit circle. To do this we introduce new variables x'' and y'' : $x' \rightarrow x'' = \frac{x'}{\sqrt{\lambda_1}}$ and $y' \rightarrow y'' = \frac{y'}{\sqrt{\lambda_2}}$, where λ_1 and λ_2 are eigenvalues from $\mathbf{D}_{(1)}$. In terms of the new coordinates, the quadratic forms are

$$(x'')^2 + (y'')^2 = (\mathbf{x}'')^t \begin{pmatrix} 1 & 0 \\ 0 & 1 \end{pmatrix} \mathbf{x}'' \leq 1, \quad (17)$$

$$f(x'', y'') = \frac{1}{\sqrt{2}}(x'')^2 - \sqrt{2}(y'')^2 - 2x''y'' = (\mathbf{x}'')^t \begin{pmatrix} \frac{1}{\sqrt{2}} & -1 \\ -1 & -\sqrt{2} \end{pmatrix} \mathbf{x}''. \quad (18)$$

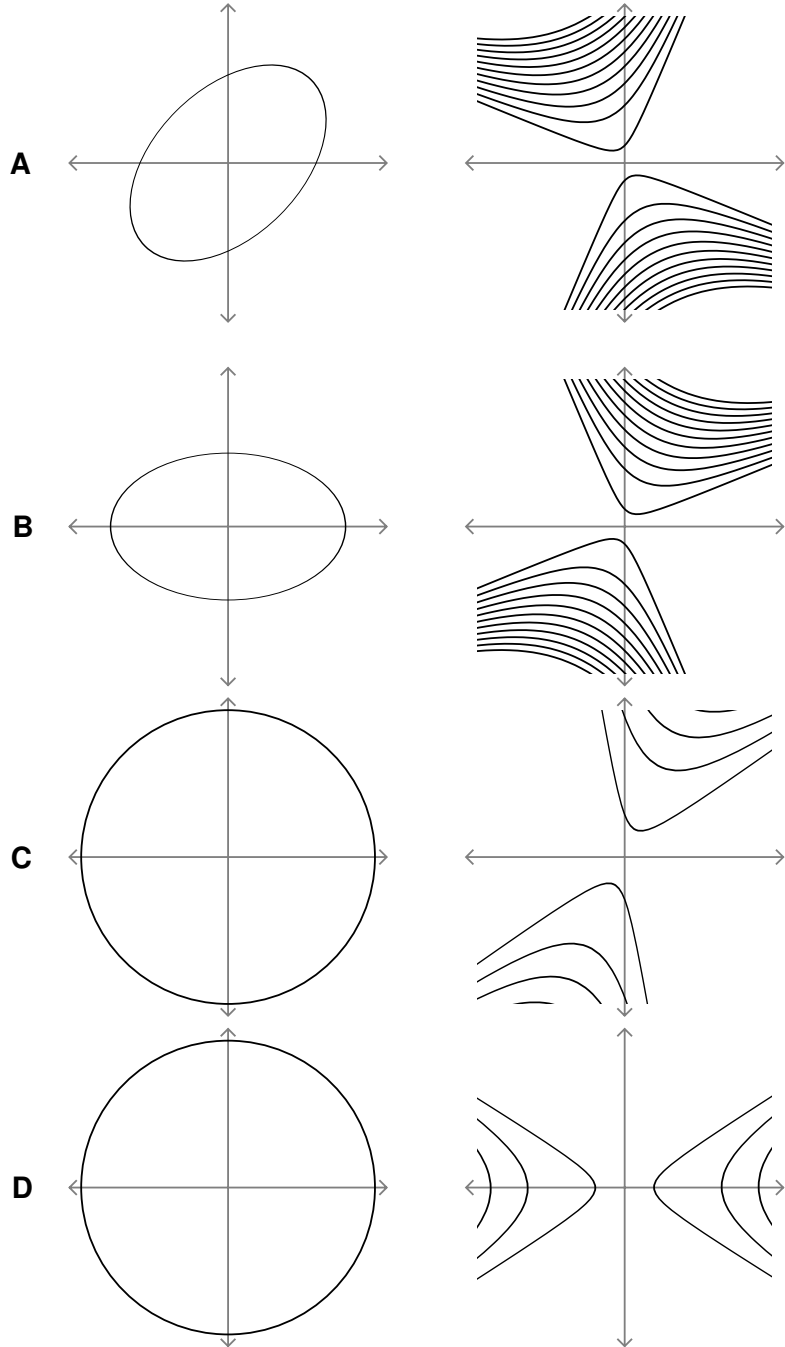


Figure 4: Geometric demonstration of joint diagonalization of the quadratic forms (panel A) $1 = \frac{3}{4}x^2 + \frac{3}{4}y^2 + \frac{1}{2}xy$ (left), and $f(x, y) = \frac{1}{\sqrt{2}}x^2 - \frac{1}{\sqrt{2}}y^2 + \sqrt{2}xy$ (right). There are three steps to the joint diagonalization: (panel B) diagonalization of the ellipse, (panel C) stretching the ellipse along the x and y to axis to the unit circle, and (panel D) diagonalization the second quadratic form.

Now we have two quadratic forms (17) and (18) where the constraint has been diagonalized and rescaled to the unit circle (the transformation symmetrizes the ellipse), and the second quadratic form has had a change of basis and a linear rescaling but remains in a non-diagonalized form.

Can we diagonalize the second quadratic form while keeping the quadratic constraint unchanged? The answer is yes, once it is a circle, it can be rotated in any direction and it remains the same circle. It is the special nature of the unit circle that allows a quadratic form to be invariant under a change in basis. It is easy to see why. Let $\mathbf{x}^t \mathbf{I} \mathbf{x}$ be a quadratic form of the unit sphere. The matrix \mathbf{I} consists of ones on the diagonal and zeros everywhere else. A matrix with this structure is known as the identity matrix because, if \mathbf{A} is a matrix of the same dimension, then $\mathbf{A}\mathbf{I} = \mathbf{A} = \mathbf{I}\mathbf{A}$. If we had wanted to change the basis of \mathbf{I} by \mathbf{K} , an orthonormal basis for the same degree quadratic form, then

$$\mathbf{K}^{-1} \mathbf{I} \mathbf{K} = (\mathbf{K}^{-1} \mathbf{I}) \mathbf{K} = \mathbf{K}^{-1} \mathbf{K} = \mathbf{I}.$$

Therefore when we change the basis we always get the same quadratic form back $\mathbf{x}^t \mathbf{I} \mathbf{x} = \mathbf{x}^t \mathbf{x}$.

If we diagonalize the second quadratic form we obtain a new orthonormal basis $\beta_{(4)} = \{\mathbf{e}_1 = (0.3690, 0.9294), \mathbf{e}_2 = (-0.9294, 0.3690)\}$. (At this point the eigenvectors and eigenvalues cannot be represented succinctly as fractions so we will continue by using fixed precision. The change of basis corresponds to a rotation of 1.19 radians (68.3°) around the origin. Along with the eigenvectors, we have the eigenvalues $\lambda_1 = \frac{-\sqrt{2}+\sqrt{34}}{4} \approx -1.811$ and $\lambda_2 = \frac{-\sqrt{2}-\sqrt{34}}{4} \approx 1.104$. The quadratic forms finally appear as

$$(x''')^2 + (y''')^2 = (\mathbf{x}''')^t \begin{pmatrix} 1 & 0 \\ 0 & 1 \end{pmatrix} \mathbf{x}''' = 1, \quad (19)$$

$$f(x''', y''') = -1.811(x''')^2 + 1.104(y''')^2 = (\mathbf{x}''')^t \begin{pmatrix} -1.811 & 0 \\ 0 & 1.104 \end{pmatrix} \mathbf{x}'''. \quad (20)$$

The last step is to find the smallest and largest values of the function (20) over the uncertain inputs specified by the ellipse (19), which because of the transformations has become a sphere. A quadratic function can easily be maximized or minimized on the unit sphere $\mathbf{x}^t \mathbf{I} \mathbf{x} = 1$. The largest eigenvalue is the maximum the function reaches under the constraint and the smallest eigenvalue is the minimum reached by the function under the constraint. In the case of (14), there is no global minimum or maximum for the function. The function will reach its extrema on the surface of unit sphere. Therefore the constraint is more general and can be changed to an inequality $\mathbf{x}^t \mathbf{I} \mathbf{x} \leq 1$. The maximum value the function reaches under the elliptical constraint is 1.104 and minimum value is -1.811. Thus, the range of the function (14) over the inputs specified by (13) is the interval [-1.811, 1.104].

6 Finding the range of a quadratic function over an ellipsoid

As we described earlier, we must find the maximum and the minimum of the given quadratic function

$$f(x_1, \dots, x_n) = f_0 + \sum_{i=1}^n f_i \cdot x_i + \sum_{i=1}^n \sum_{j=1}^n f_{i,j} \cdot x_i \cdot x_j \quad (21)$$

over the given ellipsoid

$$\sum_{i=1}^n \sum_{j=1}^n a_{i,j} \cdot (x_i - \tilde{x}_i) \cdot (x_j - \tilde{x}_j) \leq 1. \quad (22)$$

As we have just learned, we can easily extract the values \tilde{x}_i from the experts; however, we do not directly get the values $a_{i,j}$ from the experts, we only get the matrix $z_{i,j}$ that is the inverse to the matrix $a_{i,j}$. For simplicity, we will assume we already know the inverse matrix $a_{i,j}$. After we describe the main idea for this simplified case, we will then discuss what to do when we only know $z_{i,j}$.

Let us start with the analysis of the constrained optimization problem (21)–(22). In general, the difficulty in solving the constrained optimization problems comes either from the objective function itself being difficult to optimize or the constraints being difficult to take into consideration. In our case, the objective function is quadratic. If we did not have any constraints, then, to find its optima, we could simply differentiate f with respect to each of n variables and equate all n derivatives to 0. The derivative of a quadratic function is a linear function. Thus, in the absence of constraints, we would have a system of n linear equations with n unknown, a system that is easy to solve.

In contrast to the general case of constrained optimization discussed in section ??, in our specific case embodied in expressions (21)–(22), the main difficulty lies not in the objective function (21), but in the constraints (22). Therefore, a natural strategy for solving our optimization problem would be to first try to simplify the constraints as much as possible and, only when there is no possibility to further simplify the constraints, to simplify the objective function as well.

We have already discussed the first simplification of (22), which is the introduction of new variables $\Delta x_i = x_i - \tilde{x}_i$. In these new variables, the constraints (22) take the simplified form

$$\sum_{i=1}^n \sum_{j=1}^n a_{i,j} \cdot \Delta x_i \cdot \Delta x_j \leq 1. \quad (23)$$

To describe the objective function in terms of the new variables Δx_i , we must also substitute the expression $x_i = \tilde{x}_i + \Delta x_i$ into formula (21). As a result, we obtain

the expression

$$f(x_1, \dots, x_n) = f'_0 + \sum_{i=1}^n f'_i \cdot \Delta x_i + \sum_{i=1}^n \sum_{j=1}^n f_{i,j} \cdot \Delta x_i \cdot \Delta x_j, \quad (24)$$

where

$$f'_0 = f_0 + \sum_{i=1}^n f_i \cdot \tilde{x}_i + \sum_{i=1}^n \sum_{j=1}^n f_{i,j} \cdot \tilde{x}_i \cdot \tilde{x}_j, \quad (25)$$

and

$$f'_i = f_i + 2 \cdot \sum_{j=1}^n f_{i,j} \cdot \tilde{x}_j. \quad (26)$$

A detailed description of the derivation of this and other formulas is given in Appendix 2.

How can we further simplify expression (23)? The expression contains a general quadratic form $\sum a_{i,j} \cdot \Delta x_i \cdot \Delta x_j$. In expression (23) each n -dimensional vector $\Delta \mathbf{x} = (\Delta x_1, \dots, \Delta x_n)$ is described by its coordinates in the standard coordinate system with respect to the standard basis formed by n mutually orthogonal unit vectors $\mathbf{e}^{(1)} = (1, 0, \dots, 0)$, $\mathbf{e}^{(2)} = (0, 1, 0, \dots, 0)$, \dots , $\mathbf{e}^{(n)} = (0, \dots, 0, 1)$:

$$\Delta \mathbf{x} = \Delta x_1 \cdot \mathbf{e}^{(1)} + \dots + \Delta x_n \cdot \mathbf{e}^{(n)}. \quad (27)$$

Using scalar dot product of two vectors to multiply both sides of formula (27) by $\mathbf{e}^{(i)}$, and taking into consideration that $\mathbf{e}^{(i)}$ is an orthonormal basis, i.e., $\mathbf{e}^{(i)} \cdot \mathbf{e}^{(j)} = 0$ for $i \neq j$ and $\mathbf{e}^{(i)} \cdot \mathbf{e}^{(i)} = 1$, we conclude that $\Delta x_i = \Delta \mathbf{x} \cdot \mathbf{e}^{(i)}$. The i th coefficient Δx_i in the expansion (27) can be therefore described as the results of scalar product of the vector $\Delta \mathbf{x}$ and the corresponding vector $\mathbf{e}^{(i)}$ from the orthonormal basis.

It is known (see, e.g., Golub and Loan 1996) that an arbitrary quadratic form can be simplified by *diagonalization* using a different basis of n mutually orthogonal unit vectors, namely, the basis formed by unit eigenvectors $\mathbf{v}^{(1)} = (v_1^{(1)}, \dots, v_n^{(1)})$, \dots , $\mathbf{v}^{(n)} = (v_1^{(n)}, \dots, v_n^{(n)})$ of the matrix \mathbf{A} , i.e., vectors for which $\mathbf{A} \cdot \mathbf{v}^{(k)} = \lambda_k \cdot \mathbf{v}^{(k)}$ for some real numbers λ_k (called *eigenvalues*). When all the eigenvalues are different, the corresponding eigenvectors are mutually orthogonal. In the degenerate case, when some eigenvalues coincide, the eigenvectors corresponding to the equal eigenvalues are not necessarily orthogonal. In this case, however, we can apply an appropriate orthonormalization procedure and obtain mutually orthogonal vectors. Because we can use a procedure for computing eigenvalues and eigenvectors that always returns mutually orthogonal eigenvectors, we will assume that different eigenvectors are orthogonal to each other.

If, to describe a vector $\Delta \mathbf{x}$, we use its coordinates with respect to the new basis, i.e., the values y_1, \dots, y_n such that

$$\Delta \mathbf{x} = y_1 \cdot \mathbf{v}^{(1)} + \dots + y_n \cdot \mathbf{v}^{(n)},$$

then the quadratic form $\sum a_{i,j} \cdot \Delta x_i \cdot \Delta x_j$ turns into a simpler expression $\sum \lambda_k^2 \cdot y_k^2$ in terms of the new coordinates. Thus, constraint (23) simplifies to

$$\sum_{k=1}^n \lambda_k^2 \cdot y_k^2 \leq 1. \quad (28)$$

To describe the objective function (24) in terms of the new variables, we can use the fact that

$$\Delta x_i = \sum_{k=1}^n v_i^{(k)} \cdot y_k. \quad (29)$$

See Appendix 2 for the derivation of this fact. Substituting expression (29) into objective function (24), we conclude that

$$f(x_1, \dots, x_n) = f'_0 + \sum_{k=1}^n g_k \cdot y_k + \sum_{k=1}^n \sum_{l=1}^n g_{k,l} \cdot y_k \cdot y_l, \quad (30)$$

where

$$g_k = \sum_{i=1}^n f'_i \cdot v_i^{(k)} \quad (31)$$

and

$$g_{k,l} = \sum_{i=1}^n \sum_{j=1}^n f_{i,j} \cdot v_i^{(k)} \cdot v_j^{(l)}. \quad (32)$$

The problem is now to optimize the quadratic function (30) under the simplified quadratic constraint (29).

Can we simplify the constraint (29) even further? Yes, if, instead of the original variables y_k , we introduce new variables $z_k = \sqrt{\lambda_k} \cdot y_k$ for which $z_k^2 = \lambda_k \cdot y_k^2$ and therefore, constraint (24) takes an even simpler form

$$\sum_{k=1}^n z_k^2 \leq 1. \quad (33)$$

This simplification represents completing the square for each dimension. Geometrically, this constraint describes a unit sphere in n -dimensional space.

Substituting $y_k = \frac{z_k}{\sqrt{\lambda_k}}$ into the expression (30) for the objective function, we get the new expression

$$f(x_1, \dots, x_n) = f'_0 + \sum_{k=1}^n g'_k \cdot z_k + \sum_{k=1}^n \sum_{l=1}^n g'_{k,l} \cdot z_k \cdot z_l, \quad (34)$$

where

$$g'_k \stackrel{\text{def}}{=} \frac{g_k}{\sqrt{\lambda_k}}; \quad g'_{k,l} \stackrel{\text{def}}{=} \frac{g_{k,l}}{\sqrt{\lambda_k} \cdot \sqrt{\lambda_l}}. \quad (35)$$

Because the constraints have the simplest possible form, the only way to make the problem easier to solve is to simplify the objective function. We already know how to simplify the quadratic form using the eigenvalues μ_k and eigenvectors $\mathbf{u}^{(p)} = (u_1^{(p)}, \dots, u_n^{(p)})$ of the matrix $g'_{k,l}$. In terms of the new variables

$$t_p = \sum_{k=1}^n u_k^{(p)} \cdot y_k, \quad (36)$$

constraint (33) retains its form

$$\sum_{p=1}^n t_p^2 \leq 1; \quad (37)$$

(see Appendix 2 for details) while the objective function simplifies to

$$f(x_1, \dots, x_n) = f'_0 + \sum_{p=1}^n h_p \cdot t_p + \sum_{p=1}^n \mu_p \cdot t_p^2, \quad (38)$$

where

$$h_p \stackrel{\text{def}}{=} \sum_{k=1}^n u_k^{(p)} \cdot g_k. \quad (39)$$

After all the above simplification steps, we arrive at a problem of optimizing objective function (38) under the constraint (37). To solve this problem, we will use the Lagrange multiplier technique. The idea behind the Lagrange multiplier approach to finding the optimum (minimum or maximum) of an objective function f under the constraint $g \leq 1$ is that the optimum is attained either inside the constraint set S , or on its border. If the optimum is attained inside the set S , then it is a local or global optimum of the function f , so the gradient of f is equal to 0 at this point. If the optimum is attained on the border of the set S , i.e., at the point where $g = 1$, then we should look for unconstrained optima of the function $f + \lambda \cdot g$, where the value of the Lagrange multiplier λ is determined from the condition that $g = 1$. This means that we should consider any unconstrained optima of the objective function f that satisfy the constraint $g \leq 1$. We must also look for the optima of the function $f + \lambda \cdot g$. In our case, the objective function is described by formula (38) and the constraint by formula (37). Differentiating (38) w.r.t. t_p and setting the derivative to 0, we conclude that $h_p + 2\mu_p \cdot t_p = 0$, or

$$t_p = -\frac{h_p}{2\mu_p}. \quad (40)$$

Similarly, for the function $f + \lambda \cdot g$, we conclude that $h_p + 2(\mu_p + \lambda) \cdot t_p = 0$, so that, for $\lambda \neq -\mu_p$,

$$t_p = -\frac{h_p}{2 \cdot (\mu_p + \lambda)}, \quad (41)$$

in which case the condition (37) turns into

$$\sum_{p=1}^n \frac{h_p^2}{4 \cdot (\mu_p + \lambda)^2} = 1. \quad (42)$$

This equation could then be used for determining λ . We can solve this nonlinear equation with one unknown λ by applying one of the standard algorithms for solving such equations that are well described in numerical methods textbooks (see, e.g., Gerald and Wheatley 2004), such as bisection, Newton's method, secants method, etc. Once λ is found, we can compute the corresponding values t_p by using formula (41).

Equation (41) describes the *general case*, when $h_p \neq 0$ and thus, the case $\lambda = -\mu_p$ is impossible. In practice, we can also have a *degenerate case* in which, for some p , we have $\lambda = -\mu_p$ and $h_p = 0$. For this λ and this p , we can uniquely determine t_q for all $q \neq p$, but for this particular p , the equation $h_p + 2(\mu_p + \lambda) \cdot t_p = 0$ is satisfied for every real number t_p . In this degenerate case, we can find t_p from the condition that $t_1^2 + \dots + t_n^2 = 1$ using

$$t_p = \pm \sqrt{1 - \sum_{q \neq p} t_q^2}.$$

For each selected combination $t = (t_1, \dots, t_p)$, we compute the value of the objective function (38). The largest of the computed values is the maximum of f under the constraint, the smallest of these values is the minimum of f under this same constraint.

To complete our description, we must now explain what to do if, instead of the actual matrix \mathbf{A} , we only know the inverse matrix $\mathbf{Z} = \mathbf{A}^{-1}$. In this case, what we suggest to do is to find eigenvalues and eigenvectors of the matrix \mathbf{Z} . One can easily check that the matrices \mathbf{A} and \mathbf{Z} have exactly the same eigenvectors $\mathbf{v}^{(k)}$; the only difference is that for each eigenvector, the corresponding eigenvalue $\lambda_k^{(z)}$ of the matrix \mathbf{Z} is a reciprocal of the eigenvalue λ_k for the matrix \mathbf{A} : $\lambda_k^{(z)} = \frac{1}{\lambda_k}$. Thus, after finding the eigenvalues $\lambda_k^{(z)}$ of the matrix \mathbf{Z} , we would then compute the values λ_k as $\lambda_k = \frac{1}{\lambda_k^{(z)}}$.

6.1 Algorithm

In this algorithm, we start with the coefficients f_0 , f_i , and $f_{i,j}$ that describe the quadratic objective function

$$f(x_1, \dots, x_n) = f_0 + \sum_{i=1}^n f_i \cdot x_i + \sum_{i=1}^n \sum_{j=1}^n f_{i,j} \cdot x_i \cdot x_j, \quad (21)$$

and with the values \tilde{x}_i and $z_{i,j}$ that characterize the constraint

$$\sum_{i=1}^n \sum_{j=1}^n a_{i,j} \cdot (x_i - \tilde{x}_i) \cdot (x_j - \tilde{x}_j) \leq 1, \quad (22)$$

in which the matrix $A = (a_{i,j})$ is the inverse to the matrix $\mathbf{Z} = (z_{i,j})$. To find the optima of the function (21) under the constraint (22), we should do the following:

- First, we compute the values f'_0 and f'_i by using the formulas (25) and (26).
- Then, we compute the eigenvalues $\lambda_1^{(z)}, \dots, \lambda_n^{(z)}$ of the matrix \mathbf{Z} and the corresponding eigenvectors

$$\mathbf{v}^{(1)} = (v_1^{(1)}, \dots, v_n^{(1)}), \dots, \mathbf{v}^{(n)} = (v_1^{(n)}, \dots, v_n^{(n)}).$$

- After that, for k from 1 to n , we compute $\lambda_k = \frac{1}{\lambda_k^{(z)}}$.
- Next, we compute the values g_k and $g_{k,l}$ by using the formulas (31) and (32).
- We compute the values g'_k and $g'_{k,l}$ by using the formula (35).
- Then, we compute the eigenvalues μ_1, \dots, μ_n of the matrix $(g'_{k,l})$ and the corresponding eigenvectors

$$\mathbf{u}^{(1)} = (u_1^{(1)}, \dots, u_n^{(1)}), \dots, \mathbf{u}^{(n)} = (u_1^{(n)}, \dots, u_n^{(n)}).$$

- After that, we compute the value h_p by using the formula (39).
- Then, we compute the values t_p by using the formula (40), and check whether $\sum t_p^2 \leq 1$. If this inequality is satisfied, we compute the corresponding value (38).
- After that, we solve the equation (42) with the unknown λ and, for each resulting λ , compute the value t_p by using the formula (41), and then the corresponding value of the objective function (38).
- Finally, we find the smallest and the largest of the computed values (38):
 - the smallest of these values is the minimum of (21) under the constraint (22); and
 - the largest of these values is the maximum of (21) under the constraint (22).

6.2 Simple numerical example (continued)

To illustrate how this algorithm works, let us consider the same set S as in the previous numerical example (where we illustrated how to elicit the ellipsoid from an expert). In this case, $n = 2$, $\tilde{x}_1 = \tilde{x}_2 = 0$, and the matrix \mathbf{Z} has the form:

$$\mathbf{Z} = \begin{pmatrix} 4/3 & 2/3 \\ 2/3 & 4/3 \end{pmatrix}.$$

Since we considered the case when the parameters x_1 and x_2 are correlated, it is reasonable to assume that for the objective function, these parameters are interdependent. As an example of such interdependence, let us take the objective function $f(x_1, x_2) = (x_1 - x_2)^2$, i.e., $f(x_1, x_2) = x_1^2 - 2x_1 \cdot x_2 + x_2^2$. In this case, $f_0 = 0$, $f_1 = f_2 = 0$, and the matrix $f_{i,j}$ has the following form:

$$(f_{i,j}) = \begin{pmatrix} 1 & -1 \\ -1 & 1 \end{pmatrix}.$$

According to our algorithm, first, we compute the values f'_0 and f'_i by using the formulas

$$f'_0 = f_0 + \sum_{i=1}^n f_i \cdot \tilde{x}_i + \sum_{i=1}^n \sum_{j=1}^n f_{i,j} \cdot \tilde{x}_i \cdot \tilde{x}_j, \quad (25)$$

and

$$f'_i = f_i + 2 \cdot \sum_{j=1}^n f_{i,j} \cdot \tilde{x}_j. \quad (26)$$

In our case, since $\tilde{x}_1 = \tilde{x}_2 = f_0 = f_1 = f_2 = 0$, we end up with $f'_0 = 0$, $f'_1 = 0$, and $f'_2 = 0$.

Then, we compute the eigenvalues $\lambda_1^{(z)}, \lambda_2^{(z)}$ of the matrix \mathbf{Z} and the corresponding eigenvectors $\mathbf{v}^{(1)} = (v_1^{(1)}, \dots, v_n^{(1)})$ and $\mathbf{v}^{(2)} = (v_1^{(2)}, \dots, v_n^{(2)})$. By definition of an eigenvector, since $\mathbf{Z}\mathbf{v}^{(k)} = \lambda^{(z)} \cdot \mathbf{v}^{(k)}$, it means that

$$(\mathbf{Z} - \lambda_k^{(z)} \cdot \mathbf{I})\mathbf{v}^{(k)} = 0, \quad (43)$$

where \mathbf{I} denotes the unit matrix. Since the linear system of equations (43) with 0 right-hand side has a nonzero solution $\mathbf{v}^{(k)} \neq 0$, it means that this system is degenerate, i.e., that the determinant $\det(\mathbf{Z} - \lambda_k^{(z)} \cdot \mathbf{I})$ of the corresponding matrix is equal to 0. In our case, this determinant is equal to

$$\det \begin{pmatrix} 4/3 - \lambda_k^{(z)} & 2/3 \\ 2/3 & 4/3 - \lambda_k^{(z)} \end{pmatrix} = \left(\frac{4}{3} - \lambda_k^{(z)}\right)^2 - \left(\frac{2}{3}\right)^2,$$

so by equating this determinant to 0, we conclude that

$$\left(\frac{4}{3} - \lambda_k^{(z)}\right)^2 = \left(\frac{2}{3}\right)^2.$$

Hence,

$$\frac{4}{3} - \lambda_k^{(z)} = \pm \frac{2}{3}$$

and

$$\lambda_k^{(z)} = \frac{4}{3} \mp \frac{2}{3}.$$

Thus, we have two eigenvalues:

$$\lambda_1^{(z)} = \frac{2}{3}; \quad \lambda^{(z)} = 2.$$

For the first eigenvalue $\lambda_1^{(z)} = \frac{2}{3}$, we have

$$\mathbf{Z} - \lambda_1^{(z)} \cdot \mathbf{I} = \begin{pmatrix} 4/3 - 2/3 & 2/3 \\ 2/3 & 4/3 - 2/3 \end{pmatrix} = \begin{pmatrix} 2/3 & 2/3 \\ 2/3 & 2/3 \end{pmatrix}.$$

Thus, the condition $(\mathbf{Z} - \lambda_1^{(z)})\mathbf{v}^{(1)} = 0$ means that $\mathbf{v}_1^{(1)} + \mathbf{v}_2^{(1)} = 0$, i.e., that $\mathbf{v}_2^{(1)} = -\mathbf{v}_1^{(1)}$. Since the vector $\mathbf{v}^{(1)}$ must be a unit vector, we must have

$$(\mathbf{v}_1^{(1)})^2 + (\mathbf{v}_2^{(1)})^2 = 1.$$

Since $(\mathbf{v}_1^{(1)})^2 = (\mathbf{v}_2^{(1)})^2$, we thus conclude that $(\mathbf{v}_1^{(1)})^2 = \frac{1}{2}$, hence $\mathbf{v}_1^{(1)} = \frac{1}{\sqrt{2}}$.

From $\mathbf{v}_2^{(1)} = -\mathbf{v}_1^{(1)}$, we can now conclude that $\mathbf{v}_2^{(1)} = -\frac{1}{\sqrt{2}}$.

For the second eigenvalue $\lambda_2^{(z)} = 2$, we have

$$\mathbf{Z} - \lambda_2^{(z)} \cdot \mathbf{I} = \begin{pmatrix} 4/3 - 2 & 2/3 \\ 2/3 & 4/3 - 2 \end{pmatrix} = \begin{pmatrix} -2/3 & 2/3 \\ 2/3 & -2/3 \end{pmatrix}.$$

Thus, the condition $(\mathbf{Z} - \lambda_2^{(z)})\mathbf{v}^{(2)} = 0$ means that $-\mathbf{v}_1^{(2)} + \mathbf{v}_2^{(2)} = 0$, i.e., that $\mathbf{v}_2^{(2)} = \mathbf{v}_1^{(2)}$. Since the vector $\mathbf{v}^{(2)}$ must be a unit vector, we must have

$$(\mathbf{v}_1^{(2)})^2 + (\mathbf{v}_2^{(2)})^2 = 1.$$

Since $(\mathbf{v}_1^{(2)})^2 = (\mathbf{v}_2^{(2)})^2$, we thus conclude that $(\mathbf{v}_1^{(2)})^2 = \frac{1}{2}$, hence $\mathbf{v}_1^{(2)} = \frac{1}{\sqrt{2}}$.

From $\mathbf{v}_2^{(2)} = \mathbf{v}_1^{(2)}$, we can now conclude that $\mathbf{v}_2^{(2)} = \frac{1}{\sqrt{2}}$. So:

$$\mathbf{v}^{(1)} = \left(\frac{1}{\sqrt{2}}, -\frac{1}{\sqrt{2}} \right), \quad \mathbf{v}^{(2)} = \left(\frac{1}{\sqrt{2}}, \frac{1}{\sqrt{2}} \right).$$

After that, for k from 1 to n , we compute $\lambda_k = \frac{1}{\lambda_k^{(z)}}$. In our case, we get

$$\lambda_1 = \frac{3}{2}; \quad \lambda_2 = \frac{1}{2}.$$

Next, we compute the values g_k and $g_{k,l}$ by using the formulas

$$g_k = \sum_{i=1}^n f'_i \cdot v_i^{(k)} \quad (31)$$

and

$$g_{k,l} = \sum_{i=1}^n \sum_{j=1}^n f_{i,j} \cdot v_i^{(k)} \cdot v_j^{(l)}. \quad (32)$$

In our case, $f'_1 = f'_2 = 0$, so the formula (31) leads to $g_1 = g_2 = 0$. For (32), we get:

$$g_{1,1} = f_{1,1} \cdot v_1^{(1)} \cdot v_1^{(1)} + f_{1,2} \cdot v_1^{(1)} \cdot v_2^{(1)} + f_{2,1} \cdot v_2^{(1)} \cdot v_1^{(1)} + f_{2,2} \cdot v_2^{(1)} \cdot v_2^{(1)} =$$

$$1 \cdot \frac{1}{\sqrt{2}} \cdot \frac{1}{\sqrt{2}} + (-1) \cdot \frac{1}{\sqrt{2}} \cdot \left(-\frac{1}{\sqrt{2}}\right) + (-1) \cdot \left(-\frac{1}{\sqrt{2}}\right) \cdot \frac{1}{\sqrt{2}} + 1 \cdot \left(-\frac{1}{\sqrt{2}}\right) \cdot \left(-\frac{1}{\sqrt{2}}\right) =$$

$$\frac{1}{2} + \frac{1}{2} + \frac{1}{2} + \frac{1}{2} = 2;$$

$$g_{1,2} = g_{21} = f_{1,1} \cdot v_1^{(1)} \cdot v_1^{(2)} + f_{1,2} \cdot v_1^{(1)} \cdot v_2^{(2)} + f_{2,1} \cdot v_2^{(1)} \cdot v_1^{(2)} + f_{2,2} \cdot v_2^{(1)} \cdot v_2^{(2)} =$$

$$1 \cdot \frac{1}{\sqrt{2}} \cdot \frac{1}{\sqrt{2}} + (-1) \cdot \frac{1}{\sqrt{2}} \cdot \frac{1}{\sqrt{2}} + (-1) \cdot \left(-\frac{1}{\sqrt{2}}\right) \cdot \frac{1}{\sqrt{2}} + 1 \cdot \left(-\frac{1}{\sqrt{2}}\right) \cdot \frac{1}{\sqrt{2}} =$$

$$\frac{1}{2} - \frac{1}{2} + \frac{1}{2} - \frac{1}{2} = 0;$$

$$g_{2,2} = f_{1,1} \cdot v_1^{(2)} \cdot v_1^{(2)} + f_{1,2} \cdot v_1^{(2)} \cdot v_2^{(2)} + f_{2,1} \cdot v_2^{(2)} \cdot v_1^{(2)} + f_{2,2} \cdot v_2^{(2)} \cdot v_2^{(2)} =$$

$$1 \cdot \frac{1}{\sqrt{2}} \cdot \frac{1}{\sqrt{2}} + (-1) \cdot \frac{1}{\sqrt{2}} \cdot \frac{1}{\sqrt{2}} + (-1) \cdot \frac{1}{\sqrt{2}} \cdot \frac{1}{\sqrt{2}} + 1 \cdot \frac{1}{\sqrt{2}} \cdot \frac{1}{\sqrt{2}} =$$

$$\frac{1}{2} - \frac{1}{2} - \frac{1}{2} + \frac{1}{2} = 0.$$

So, the matrix $(g_{k,l})$ takes the following form:

$$(g_{k,l}) = \begin{pmatrix} 2 & 0 \\ 0 & 0 \end{pmatrix}.$$

We compute the values g'_k and $g'_{k,l}$ by using the formula

$$g'_k = \frac{g_k}{\sqrt{\lambda_k}}; \quad g'_{k,l} = \frac{g_{k,l}}{\sqrt{\lambda_k} \cdot \sqrt{\lambda_l}}. \quad (35)$$

Since $g_1 = g_2 = 0$, we get $g'_1 = g'_2 = 0$. Similarly, since the only nonzero element $g_{k,l}$ is the element $g_{1,1}$, the only nonzero element of the matrix $g'_{k,l}$ is also $g'_{1,1}$:

$$g'_{1,1} = \frac{g_{1,1}}{\sqrt{\lambda_1} \cdot \sqrt{\lambda_1}} = \frac{2}{\sqrt{3/2} \cdot \sqrt{3/2}} = \frac{2}{3/2} = \frac{4}{3}.$$

Therefore, the matrix $g'_{k,l}$ takes the following form:

$$(g'_{k,l}) = \begin{pmatrix} 4/3 & 0 \\ 0 & 0 \end{pmatrix}.$$

Then, we compute the eigenvalues μ_1, μ_2 of the matrix $(g'_{k,l})$ and the corresponding eigenvectors $\mathbf{u}^{(1)} = (u_1^{(1)}, u_2^{(1)})$ and $\mathbf{u}^{(2)} = (u_1^{(2)}, u_2^{(2)})$. Since the matrix $g'_{k,l}$ is already in the diagonal form, the coordinate unit vectors are its eigenvectors, and the diagonal elements are its eigenvalues:

$$u^{(1)} = (1, 0); \quad u^{(2)} = (0, 1); \quad \mu_1 = \frac{4}{3}; \quad \mu_2 = 0.$$

After that, we compute the value h_p by using the formula

$$h_p = \sum_{k=1}^n u_k^{(p)} \cdot g_k. \quad (39)$$

In our case, $g_1 = g_2 = 0$, hence $h_1 = h_2 = 0$.

Then, we compute the values t_p by using the formula

$$t_p = -\frac{h_p}{2\mu_p}. \quad (40)$$

In our case, $h_1 = h_2 = 0$, hence $t_1 = t_2 = 0$. We then check whether the inequality

$$\sum_{p=1}^n t_p^2 \leq 1 \quad (37)$$

is satisfied. We have $t_1^2 + t_2^2 = 0 \leq 1$, so this inequality is indeed satisfied. Since the inequality (37) is satisfied, we compute the corresponding value

$$f(x_1, \dots, x_n) = f'_0 + \sum_{p=1}^n h_p \cdot t_p + \sum_{p=1}^n \mu_p \cdot t_p^2. \quad (38)$$

In our case, $f'_0 = 0$, $t_1 = t_2 = 0$, $\mu_1 = \frac{4}{3}$, and $\mu_2 = 0$, hence

$$f(x_1, \dots, x_n) = \frac{4}{3} \cdot t_1^2.$$

For $t = (0, 0)$, the value of this objective function is 0.

After that, we solve the equation

$$\sum_{p=1}^n \frac{h_p^2}{4 \cdot (\mu_p + \lambda)^2} = 1 \quad (42)$$

with the unknown λ . Since here, $h_1 = h_2 = 0$, in the generic case, the left-hand side is always equal to 0. Thus, we have to look for possible degenerate solutions $\lambda = -\mu_p$, where $p = 1$ or $p = 2$.

For $p = 1$, we have $\lambda = -\mu_1 = -\frac{4}{3}$. In this case, we can still use the formula

$$t_p = -\frac{h_p}{2 \cdot (\mu_p + \lambda)} \quad (41)$$

to determine t_2 : we get $t_2 = 0$. We can then find t_1 from the condition

$$t_1^2 + \dots + t_n^2 = 1,$$

as $t_1 = \pm\sqrt{1 - t_2^2} = \pm 1$. Thus, we get two vectors $t = (1, 0)$ and $t = (-1, 0)$. For both vectors, the objective function (38), which takes the form $f = \left(\frac{4}{3}\right) \cdot t_1^2$, takes the value $\frac{4}{3}$.

For $p = 2$, we have $\lambda = -\mu_2 = 0$. In this case, we can still use the formula (41) to determine t_1 : we get $t_1 = 0$. We can then find t_2 from the condition $t_1^2 + \dots + t_n^2 = 1$, as $t_2 = \pm\sqrt{1 - t_1^2} = \pm 1$. Thus, we get two vectors $t = (0, 1)$ and $t = (0, -1)$. For both vectors, the objective function (38), which takes the form $f = \left(\frac{4}{3}\right) \cdot t_2^2$, takes the value 0.

We have 2 different values of the objective function (38): 0 and $\frac{4}{3}$. In accordance with our algorithm, we compute the smallest and the largest of thus computed values (38):

- the smallest of these values, 0, is the minimum of (21) under the constraint (22); and
- the largest of these values, $\frac{4}{3}$, is the maximum of (21) under the constraint (22).

So, the range of the quadratic function $f(x_1, x_2) = (x_1 - x_2)^2$ under the constraint

$$x_1^2 - x_1 \cdot x_2 + x_2^2 \leq 1 \quad (11)$$

is the interval $\left[0, \frac{4}{3}\right]$.

Now that we have the result of our computation, we can use this example to illustrate one of the above mentioned advantages of using ellipsoids to describe “correlation” between the parameters x_i . Indeed, we have mentioned that one of the objectives of replacing the original box

$$[\underline{x}_1, \bar{x}_1] \times \dots \times [\underline{x}_n, \bar{x}_n] \quad (5)$$

with its ellipsoid subset S is that this replacement will enable us to reduce the estimated range. Let us describe how big the reduction is in this particular example.

We already know, from the section in which we started this numerical example, that in our case, $\underline{x}_1 = -\frac{2}{\sqrt{3}}$, $\bar{x}_1 = \frac{2}{\sqrt{3}}$, $\underline{x}_2 = -\frac{2}{\sqrt{3}}$, and $\bar{x}_2 = \frac{2}{\sqrt{3}}$. Therefore, the box (5) takes the following form:

$$\left[-\frac{2}{\sqrt{3}}, \frac{2}{\sqrt{3}} \right] \times \left[-\frac{2}{\sqrt{3}}, \frac{2}{\sqrt{3}} \right]. \quad (44)$$

So, to see how the use of the ellipsoid reduced the range estimate, let us find what the range estimate would be if we did not reduce ourselves to the ellipsoid. In other words, let us find out the range of the function $(x_1 - x_2)^2$ on the box (44).

In general, with respect to each variable x_i , the minimum (maximum) of a function $f(x_1, \dots, x_n)$ on an interval $[\underline{x}_i, \bar{x}_i]$ is attained:

- either at the left endpoint $x_i = \underline{x}_i$,
- or at the right endpoint $x_i = \bar{x}_i$,
- or inside the interval $[\underline{x}_i, \bar{x}_i]$, in which case $\frac{\partial f}{\partial x_i} = 0$.

For each variable, we therefore have three possible situations. For our function $f(x_1, x_2) = (x_1 - x_2)^2$, there situations are: $x_i = -\frac{2}{\sqrt{3}}$, $x_i = \frac{2}{\sqrt{3}}$, and $x_1 = x_2$. By combining 3 possibilities for x_1 and 3 possibilities for x_2 , we get the following $3 \times 3 = 9$ possible parameter vectors $x = (x_1, x_2)$:

	$x_1 = -\frac{2}{\sqrt{3}}$	$x_1 = \frac{2}{\sqrt{3}}$	$x_1 = x_2$
$x_2 = -\frac{2}{\sqrt{3}}$	$\left(-\frac{2}{\sqrt{3}}, -\frac{2}{\sqrt{3}} \right)$	$\left(\frac{2}{\sqrt{3}}, -\frac{2}{\sqrt{3}} \right)$	$\left(-\frac{2}{\sqrt{3}}, -\frac{2}{\sqrt{3}} \right)$
$x_2 = \frac{2}{\sqrt{3}}$	$\left(-\frac{2}{\sqrt{3}}, \frac{2}{\sqrt{3}} \right)$	$\left(\frac{2}{\sqrt{3}}, \frac{2}{\sqrt{3}} \right)$	$\left(\frac{2}{\sqrt{3}}, \frac{2}{\sqrt{3}} \right)$
$x_1 = x_2$	$\left(-\frac{2}{\sqrt{3}}, -\frac{2}{\sqrt{3}} \right)$	$\left(\frac{2}{\sqrt{3}}, \frac{2}{\sqrt{3}} \right)$	$x_1 = x_2$

In all these 9 situations, we can compute the corresponding value of $f = (x_1 - x_2)^2$. For example, for $x = \left(\frac{2}{\sqrt{3}}, -\frac{2}{\sqrt{3}}\right)$, we have $x_1 - x_2 = \frac{4}{\sqrt{3}}$, hence $f(x_1, x_2) = (x_1 - x_2)^2 = \frac{16}{3}$. In general, we get the following 9 values:

	$x_1 = -\frac{2}{\sqrt{3}}$	$x_1 = \frac{2}{\sqrt{3}}$	$x_1 = x_2$
$x_2 = -\frac{2}{\sqrt{3}}$	0	$\frac{16}{3}$	0
$x_2 = \frac{2}{\sqrt{3}}$	$\frac{16}{3}$	0	0
$x_1 = x_2$	0	0	0

Since the minimum and the maximum of $f(x_1, x_2)$ on the box must be among these values, the minimum is the smallest of these values, and the maximum is the largest of these values, so the range of the function on the box is $\left[0, \frac{16}{3}\right]$.

We can see that this range estimate is 4 times wider than the actual range $\left[0, \frac{4}{3}\right]$. Thus, this numerical example shows that the use of ellipsoids really helps to decrease the estimate of the desired range.

6.3 Intervals of correlation

The approach to eliciting the ellipsoid from the expert described in section 4.2 is based on the assumption that the expert knows the relation between different parameters, and the expert can provide, for each possibly correlated pair (x_i, x_j) , the value $x_{i,j}$ of the parameter x_i that is most reasonable to expect when $x_j = \bar{x}_j$. It may happen that the expert believes that there is, say, a strong positive correlation between x_i and x_j but cannot pinpoint a specific value of x_i corresponding to $x_j = \bar{x}_j$. Instead, the expert may provide an *interval* $[x_{i,j}, \bar{x}_{i,j}]$ of possible values of x_i when $x_j = \bar{x}_j$ that represents the expert's uncertainty. This would correspond to a set of different ellipsoids. Because we do not know which of these ellipsoids is the right one, we must consider all of them when estimating the range of the objective function. In other words, what we need is the range of the objective function $f(x_1, \dots, x_n)$ over the *union* of all possible ellipsoids.

The main advantage of using ellipsoids is that, since the shape of an ellipsoid is described by a simple formula, it is feasible to compute the range of a quadratic function over an ellipsoid. A union of ellipsoids can have a much more complex shape than an ellipsoid. In fact, an *arbitrary* open set can be represented as a union of open ellipsoids. We have already mentioned that even for a box, the problem of finding the exact range of a quadratic function over it is generally NP-hard. So, if

we try to find the exact range of a quadratic function over an arbitrary union of ellipsoids, the problem becomes computationally intractable.

It is therefore reasonable, instead of considering arbitrary unions, to enclose the union into an appropriate ellipsoid and then estimate the range of a quadratic function over an enclosing ellipsoid.

Once we know the enclosing ellipsoid, we already know how to find the range of a quadratic function over it. The problem is how to describe this enclosing ellipsoid. In this section, we will describe techniques for such a description.

It is reasonable to assume that the center of the enclosing ellipsoid is at the same point $\tilde{x} = (\tilde{x}_1, \dots, \tilde{x}_n)$ that is formed by midpoints of the ranges of the corresponding parameters. Thus, the desired ellipsoid has the form

$$a(x_1, \dots, x_n) \stackrel{\text{def}}{=} \sum_{i=1}^n \sum_{j=1}^n a_{i,j} \cdot (x_i - \tilde{x}_i) \cdot (x_j - \tilde{x}_j) \leq 1. \quad (10)$$

We assume that we know the values \tilde{x}_i . Thus, to find the shape of the ellipsoid, we must find the coefficients $a_{i,j}$.

For some correlated pairs of parameters (x_i, x_j) , we know the interval $[\underline{x}_{i,j}, \bar{x}_{i,j}]$ of possible values of x_i when $x_j = \bar{x}_j$. How can we transform this information into the values of the coefficients $a_{i,j}$?

To explain how this can be done, let us start with the simplest 2-D case, when an ellipsoid is simply an ellipse. In this case, we know that the intersection of the enclosing ellipsoid with the line $x_2 = \bar{x}_2$ consists of the interval $[\underline{x}_{1,2}, \bar{x}_{1,2}]$. Thus, the endpoints of this interval should belong to the surface of this ellipsoid. In other words, the surface of the ellipsoid should include the points $(\underline{x}_{1,2}, \bar{x}_2)$ and $(\bar{x}_{1,2}, \bar{x}_2)$. In other words, for these points, the left-hand side of the inequality (10) should be exactly equal to 1. Since $\bar{x}_2 - \tilde{x}_2 = \Delta_2$, we conclude that:

$$a_{1,1} \cdot (\underline{x}_{1,2} - \tilde{x}_1)^2 + 2 \cdot a_{1,2} \cdot (\underline{x}_{1,2} - \tilde{x}_1) \cdot \Delta_2 + a_{2,2} \cdot \Delta_2^2 = 1; \quad (45)$$

$$a_{1,1} \cdot (\bar{x}_{1,2} - \tilde{x}_1)^2 + 2 \cdot a_{1,2} \cdot (\bar{x}_{1,2} - \tilde{x}_1) \cdot \Delta_2 + a_{2,2} \cdot \Delta_2^2 = 1. \quad (46)$$

Thus, we get two equations relating the three unknowns $a_{1,1}$, $a_{1,2}$, and $a_{2,2}$.

We can similarly ask what are the possible values of x_2 when $x_1 = \bar{x}_1$; as a result, we will get an interval $[\underline{x}_{2,1}, \bar{x}_{2,1}]$. Based on this information, we can describe two more equations relating the three unknowns:

$$a_{1,1} \cdot \Delta_1^2 + 2 \cdot a_{1,2} \cdot \Delta_1 \cdot (\underline{x}_{2,1} - \tilde{x}_2) + a_{2,2} \cdot (\underline{x}_{2,1} - \tilde{x}_2)^2 = 1; \quad (47)$$

$$a_{1,1} \cdot \Delta_1^2 + 2 \cdot a_{1,2} \cdot \Delta_1 \cdot (\bar{x}_{2,1} - \tilde{x}_2) + a_{2,2} \cdot (\bar{x}_{2,1} - \tilde{x}_2)^2 = 1. \quad (48)$$

Now, we can either select 3 out of 4 equations, or apply the least squares method to all 4 equations, and get all three desired coefficients $a_{1,1}$, $a_{1,2}$, $a_{2,2}$ that describe our ellipse.

In the general n -dimensional case, we can apply this procedure for every correlated pair of parameters (x_i, x_j) , and get a description of the corresponding ellipse

$$a_{i,i}^{(i,j)} \cdot (x_i - \tilde{x}_i)^2 + 2 \cdot a_{i,j}^{(i,j)} \cdot (x_i - \tilde{x}_i) \cdot (x_j - \tilde{x}_j) + a_{j,j}^{(i,j)} \cdot (x_j - \tilde{x}_j)^2 \leq 1. \quad (49)$$

For independent variables (x_i, x_j) , we can assume (as we did before) that $x_{i,j} = \tilde{x}_i$ and hence, the corresponding ellipse takes the form:

$$a_{i,i}^{(i,j)} \cdot (x_i - \tilde{x}_i)^2 + a_{j,j}^{(i,j)} \cdot (x_j - \tilde{x}_j)^2 \leq 1, \quad (50)$$

where $a_{i,i}^{(i,j)} = \Delta_i^{-2}$ and $a_{j,j}^{(i,j)} = \Delta_j^{-2}$. Thus, for every two parameters x_i and x_j , we know how to derive a projection of the desired n -dimensional enclosing ellipsoid (10) onto the 2-D plane (x_i, x_j) . How can we reconstruct the ellipsoid from its projections?

It is possible to check that if we go from the matrix $a_{k,l}$ to the inverse matrix $z_{k,l}$, then the projection to a two-dimensional plane corresponds simply to restricting the matrix $z_{k,l}$ to the corresponding variables x_i and x_j . The algebraic proof of this fact is similar to our analysis from Appendix 1. Due to the fact that for the normal distribution, confidence sets are ellipsoids, this fact is also easy to understand in statistical terms: for the normal distribution

$$\rho(x_1, \dots, x_n) = \frac{1}{(2 \cdot \pi)^{n/2} \cdot \det(A)} \cdot \exp \left(- \sum_{i=1}^n \sum_{j=1}^n a_{i,j} \cdot (x_i - a_i) \cdot (x_j - a_j) \right),$$

The corresponding matrix $a_{i,j}$ is the inverse matrix to the covariance matrix $E[(x_i - a_i) \cdot (x_j - a_j)]$. When, instead of considering all n random variables x_i , we only consider some of them, all we have to do is restrict to covariance matrix to the corresponding variables. Therefore, to reconstruct the ellipsoid from its two-dimensional projections, we can do the following:

- First, for every i and j , we invert the corresponding matrix $a_{k,l}^{(i,j)}$ into a matrix $z_{k,l}^{(i,j)}$.
- Then, we combine the values $z_{k,l}^{(i,j)}$ into a single matrix:
 - For $i \neq j$, the value $z_{i,j}$ is only present in $z_{i,j}^{(i,j)}$, so we take $z_{i,j} = z_{i,j}^{(i,j)}$.
 - For $i = j$, the value $z_{i,i}$ occurs as $z_{i,i}^{(i,j)}$ for different $j \neq i$.

We are interested in finding the enclosing ellipsoid, i.e., the ellipsoid that, crudely speaking, contains all projected ellipses. In terms of $a_{i,i}$, the larger the value, the larger the product $a_{i,i} \cdot \Delta x_i^2$ and thus, the more restrictive is the corresponding inequality $a_{i,i} \cdot \Delta x_i^2 + \dots \leq 1$. Thus, in terms of $a_{i,i}$, if we want the most enclosing ellipsoid, we must select the *smallest* possible value of $a_{i,i}$. The values $z_{i,j}$ are inverses to $a_{i,j}$.

Thus, it is reasonable to select the *largest* possible value of $z_{i,i}$:

$$z_{i,i} = \min_{j \neq i} z_{i,j}^{(i,j)}.$$

As a result, we get the matrix $\mathbf{Z} = (z_{i,j})$ that is the inverse to the matrix $\mathbf{A} = (a_{i,j})$ that describes the desired enclosing ellipsoid. Knowing \mathbf{Z} , we can now use the algorithm described above to determine the range of a given quadratic function over the corresponding ellipsoid.

6.4 Nested families of intervals of correlation

What if the experts can provide additional information beyond simple intervals? Often, when an expert can provide us with an interval $[\underline{x}, \bar{x}]$ that is guaranteed to contain the value of some quantity x , this expert can also provide narrower intervals that contain x with different degrees of certainty α .

The corresponding family of nested intervals can be viewed in different ways. For instance, they may be interpreted as a fuzzy set (Nguyen 1996; 1999). Under this interpretation, the different intervals from the nested family can be viewed as α -cuts corresponding to different levels of uncertainty α . The family of nested intervals can also be interpreted as a particular case of a consonant (nested) Dempster-Shafer structure (Joslyn 1996), or as a multivariate analogue of a p-box (Ferson 2002; Ferson et al. 2003).

The calculations needed to handle a nested family are fairly simple. For each degree of certainty α , we can take the intervals corresponding to this degree of certainty, compute the corresponding ellipsoid, and then follow the algorithm of section 6.1 to estimate the range of the given quadratic function over this ellipsoid. As a result, for each α , we get the range estimate corresponding to this α . If the inputs are additionally *concentric* as well as nested, the computational burden is dramatically reduced further. In this case, the calculations needed for each ellipsoid are identical except for the very last step (panel D of Figure 4), allowing great computational shortcuts. Instead of a single interval range as the result, we get a nested family of interval ranges corresponding to different levels of certainty α . This nested family of intervals can be interpreted either as a fuzzy set or as a consonant Dempster-Shafer structure.

The next section considers the case where arbitrary Dempster-Shafer structures are provided as function inputs.

7 Propagating Dempster-Shafer structures

We would like to be able to propagate Dempster-Shafer structures through the quadratic response surface. This section shows that many of the methods and algorithms developed in this report for interval and ellipsoidal uncertainty extend to Dempster-Shafer structures.

A Dempster-Shafer structure is simply a collection of sets of possible values with weights for each set which add up to unity (see section 3.2). An individual set, called a focal element, could be an interval or, in the multivariate case, it could be a rectangular box or an ellipsoid. Mathematical operations on Dempster-Shafer structures can be decomposed into a collection of similar operations on each pairwise combination of the focal elements that make up the Dempster Shafer Structures (Yager 1986; Ferson et al. 2003).

For instance, the sum under independence of two Dempster-Shafer structures, represented by

$$\{ ([1, 3], 0.4), ([2, 5], 0.6) \}$$

and

$$\{ ([4, 7], 0.2), ([6, 8], 0.8) \}$$

is

$$\begin{aligned} &\{ ([1, 3] + [4, 7], 0.4 \times 0.2), ([1, 3] + [6, 8], 0.4 \times 0.8), \\ &([2, 5] + [4, 7], 0.6 \times 0.2), ([2, 5] + [6, 8], 0.6 \times 0.8) \}, \end{aligned}$$

which equals

$$\{ ([5, 10], 0.08), ([7, 11], 0.32), ([6, 12], 0.12), ([8, 13], 0.48) \}.$$

The operation involves computing sums for the Cartesian product of each possible pair of focal elements, one from the first Dempster-Shafer structure and one from the second. If there are three input structures, the Cartesian product will be three-dimensional and the number of separate interval problems it will take to finish the calculation will be the product of the numbers of focal elements in the three input Dempster-Shafer structures.

Propagating Dempster-Shafer structures through quadratic response models of black boxes can likewise be handled by reducing the problem to many interval problems in a Cartesian product formed by the focal elements of the inputs. However, propagating Dempster-Shafer structures through a response surface may be computation-intensive. In fact, if there are a large number of inputs to the model, even a modest number of focal elements per input would mean the answer will not be practically computable.

For example, suppose a model has 10 inputs and each input is represented by a Dempster-Shafer structure with 5 focal elements. Propagating these Dempster-Shafer structures through a response surface would entail solving the ellipsoid propagation problem described in section 6 many times, once for each element of the Cartesian product. In total, we would need to propagate

$$5^{10} = 9,765,625$$

separate ellipsoids through the response surface. Without reducing the number of focal elements, most practical problems would require a large amount of computation time.

It is important to emphasize that the methods described in this report will help to reduce the computational burden substantially. The use of (reduced) quadratic models for the black box and ellipsoidal representations of epistemic uncertainty can *vastly* simplify each of these interval propagation problems. Indeed, the efficiency may well make many problems involving the propagation of uncertainty in Dempster-Shafer structures computationally practical.

It is also important to reiterate that the computational expense discussed here occurs *after* the black box has been sampled and modeled. No additional runs of the black-box model are necessary to generalize from intervals to Dempster-Shafer structures. In theory, the process of propagating elements through a response surface could be made parallelizable, because each propagation is not dependent on the past elements. Only at the final step would a condensation procedure need to be used to reduce the number of focal elements to a manageable level.

Appendix 1.

Formulas for the ellipsoid from expert information

The elicitation of the multivariate ellipsoid involves two kinds of information: the breadth of intervals in each dimension and the dependencies between dimensions. From formula (10) one can see that an ellipsoid is symmetric with respect to the transformation $\Delta x_i \rightarrow -\Delta x_i$; in other words, if we start with a point inside the ellipsoid, and we change the signs of all the values Δx_i , then we get a point that is also inside the ellipsoid. So, if a value Δx_i is possible (i.e., occurs for some point within the ellipsoid), its negative $-\Delta x_i$ is also possible. Thus, the set of possible values of $\Delta x_i = x_i - \tilde{x}_i$ is symmetric with respect to 0, and hence, the set of possible values of x_i is symmetric with respect to \tilde{x}_i . Thus, the value \tilde{x}_i is a midpoint of the range of possible values of x_i . We know the range of possible values of x_i , because it is provided by an expert as an interval $[\underline{x}_i, \bar{x}_i]$. We can compute \tilde{x}_i as the midpoint of this interval directly as $(\underline{x}_i + \bar{x}_i)/2$.

Let us now consider the desired relation between x_i and x_j . Since the value \bar{x}_j is possible, the ellipsoid has an intersection with the hyperplane $x_j = \bar{x}_j$. As we increase x_j further, to a value $x_j = \bar{x}_j + \varepsilon$ for some small $\varepsilon > 0$, we leave the set of possible values of x_j and therefore, the ellipsoid has no intersection with the corresponding plane $x_j = \bar{x}_j + \varepsilon$. Thus, the plane $x_j = \bar{x}_j$ is a *tangent plane* to our ellipsoid.

An ellipsoid is strictly convex so, at any given point, it has only one point of intersection with a tangent plane. Thus, when $x_j = \bar{x}_j$, there is only one point in the ellipsoid. Therefore, when we ask the expert about the possible values of x_i when $x_j = \bar{x}_j$, we should expect not the range but rather a single value of x_i . In other words, instead of asking for a range, it makes sense to ask, for each correlated pair i and j , what is the most reasonable value of x_i when $x_j = \bar{x}_j$. We will denote this ‘most reasonable value’ by $x_{i,j}$. Figure 5 depicts an ellipse inscribed in a box specified by two correlated intervals.

By eliciting this information from the expert, we can extract E values $x_{i,j}$ corresponding to the E pairs that the expert nominated and ranked as most correlated. When there is a positive correlation between the parameters x_i and x_j , then, in accordance with our description of what positive correlation means, we expect x_i to grow with x_j . In other words, since $\bar{x}_j > \tilde{x}_j$, we expect $x_{i,j} > \tilde{x}_i$. When there is a negative correlation between the parameters x_i and x_j , then we expect x_i to decrease when x_j increases. In other words, since $\bar{x}_j > \tilde{x}_j$, we expect $x_{i,j} < \tilde{x}_i$. If there is no correlation, we expect that $x_{i,j}$ is neither larger nor smaller than \tilde{x}_i – i.e., we expect $x_{i,j} = \tilde{x}_i$. Thus, for all the pairs of parameters (x_i, x_j) that an expert considers to be independent or uncorrelated, we take $x_{i,j} = \tilde{x}_i$.

Now, for every i , we have the values \underline{x}_i , \bar{x}_i , and \tilde{x}_i , and for all pairs $i \neq j$, we know the value $x_{i,j}$ of x_i when $x_j = \bar{x}_j$. How can we transform this infor-

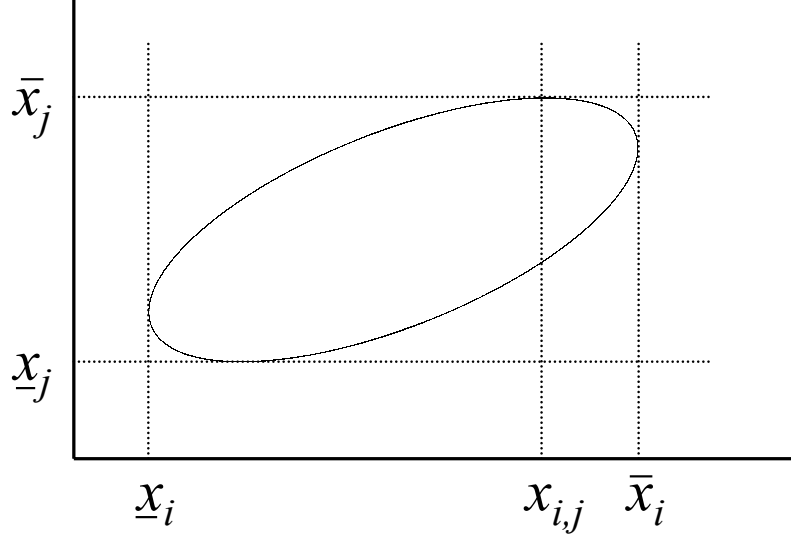


Figure 5: An ellipse inscribed within a rectangular box specified by the intervals $[\underline{x}_i, \bar{x}_i]$ and $[\underline{x}_j, \bar{x}_j]$. The dependency between x_i and x_j is determined by the point of tangency $x_{i,j}$ with the line $x_j = \bar{x}_j$. This point can be any value between \underline{x}_i and \bar{x}_i .

mation into the coefficients $a_{i,j}$ of the desired ellipsoid (10)? We have mentioned that at the point where $x_j = \bar{x}_j$, the plane $x_j = \bar{x}_j$ is a tangent to the ellipsoid. According to the definition of the values $x_{i,j}$, this means that at the point $(x_{1,j}, \dots, x_{j-1,j}, \bar{x}_j, x_{j+1,j}, \dots, x_n)$, the plane $x_j = \bar{x}_j$ is a tangent to the ellipsoid. To simplify the formulation, let us denote \bar{x}_j by $x_{j,j}$. In this new notation, the previous statement takes the following form: the plane $x_j = \bar{x}_j$ is tangent to the ellipsoid at the point with the coordinates $(x_{1,j}, \dots, x_{n,j})$.

From calculus, it is known that a tangent vector to a surface is orthogonal to its normal vector n , and the normal vector to the surface $a(x_1, \dots, x_n) = 1$ is proportional to the gradient of f , i.e., to the vector

$$\nabla a = \left(\frac{\partial a}{\partial x_1}, \dots, \frac{\partial a}{\partial x_n} \right).$$

This gradient vector is orthogonal to the plane $x_j = \bar{x}_j$, so the only nonzero com-

ponent of this gradient vector is its j th component, and all other components are 0. In other words, at the point $(x_{1,j}, \dots, x_{n,j})$, we have $\frac{\partial a}{\partial x_i} = 0$ for all $i \neq j$.

Let us use the expression (10) for the function $a(x_1, \dots, x_n)$ to find an explicit expression for this partial derivative. To do this we first separate the terms that depend on x_i and the terms that do not depend on x_i to obtain

$$a(x_1, \dots, x_n) = a_{i,i} \cdot (x_i - \tilde{x}_i)^2 + \sum_{k \neq i} a_{i,k} \cdot (x_i - \tilde{x}_i) \cdot (x_k - \tilde{x}_k) + \sum_{k \neq i} a_{k,i} \cdot (x_k - \tilde{x}_k) \cdot (x_i - \tilde{x}_i) + \sum_{k \neq i} \sum_{l \neq i} a_{k,l} \cdot (x_k - \tilde{x}_k) \cdot (x_l - \tilde{x}_l).$$

Differentiating with respect to x_i , we find that

$$\frac{\partial a}{\partial x_i} = 2a_{i,i} \cdot (x_i - \tilde{x}_i) + \sum_{k \neq i} a_{i,k} \cdot (x_k - \tilde{x}_k) + \sum_{k \neq i} a_{k,i} \cdot (x_k - \tilde{x}_k),$$

and, because $a_{i,j}$ is a symmetric matrix, that

$$\frac{\partial a}{\partial x_i} = 2a_{i,i} \cdot (x_i - \tilde{x}_i) + 2 \sum_{k \neq i} a_{i,k} \cdot (x_k - \tilde{x}_k),$$

and, finally, that

$$\frac{\partial a}{\partial x_i} = 2 \sum_{k=1}^n a_{i,k} \cdot (x_k - \tilde{x}_k).$$

At the point with coordinates $x_k = x_{k,j}$, these derivatives must be equal to 0, so

$$\sum_{k=1}^n a_{i,k} \cdot (x_{k,j} - \tilde{x}_k) = 0 \quad (\text{A1})$$

for every $i \neq j$.

The point with the coordinates $x_{1,j}, \dots, x_{n,j}$ is on the surface of the ellipsoid, so, for this point, we have $a(x_{1,j}, \dots, x_{n,j}) = 1$. Substituting the values $x_{k,j}$ into the formula (10), we conclude that

$$\sum_{i=1}^n \sum_{k=1}^n a_{i,k} \cdot (x_{i,j} - \tilde{x}_i) \cdot (x_{k,j} - \tilde{x}_k) = 1.$$

This equation can be rewritten as

$$\sum_{i=1}^n (x_{i,j} - \tilde{x}_i) \cdot \left(\sum_{k=1}^n a_{i,k} \cdot (x_{k,j} - \tilde{x}_k) \right) = 1. \quad (\text{A2})$$

Due to equation (A1), we get 0 for all $i \neq j$, and the only nonzero term is when $i = j$. Thus, in the formula (A2), we can replace the first sum with the j th term to obtain

$$(x_{j,j} - \tilde{x}_j) \cdot \left(\sum_{k=1}^n a_{j,k} \cdot (x_{k,j} - \tilde{x}_k) \right) = 1,$$

or, equivalently,

$$\sum_{k=1}^n a_{j,k} \cdot (x_{k,j} - \tilde{x}_k) \cdot \Delta_j = 1, \quad (\text{A3})$$

where $\Delta_j \stackrel{\text{def}}{=} x_{j,j} - \tilde{x}_j = \bar{x}_i - \tilde{x}_j = (\bar{x}_j - \underline{x}_j)/2$. Multiplying both sides of the equation (A1) by Δ_j , we conclude that

$$\sum_{k=1}^n a_{i,k} \cdot (x_{k,j} - \tilde{x}_k) \cdot \Delta_j = 0 \quad (\text{A4})$$

for all $i \neq j$. Equations (A3) and (A4) can be combined into a single equation

$$\sum_{k=1}^n a_{i,k} \cdot (x_{k,j} - \tilde{x}_k) \cdot \Delta_j = \delta_{i,j}, \quad (\text{A5})$$

where $\delta_{i,j} = 1$ for $i = j$ and $\delta_{i,j} = 0$ for $i \neq j$.

The formulation becomes much simpler in matrix notation. The value of $\delta_{i,j}$ are components of the unit matrix \mathbf{I} , and the sum on the left-hand side of the formula (A5) describes the product $\mathbf{A} \cdot \mathbf{X}$ of two matrices:

- the desired matrix \mathbf{A} , with components $a_{i,k}$, and
- the matrix \mathbf{Z} , with components $z_{k,j} \stackrel{\text{def}}{=} (x_{k,j} - \tilde{x}_k) \cdot \Delta_j$.

Because $\mathbf{A} \cdot \mathbf{Z} = \mathbf{I}$, $\mathbf{A} = \mathbf{Z}^{-1}$ is a solution, so we can obtain \mathbf{A} by simply inverting the matrix \mathbf{Z} .

Appendix 2.

Formulas to optimize quadratic functions over ellipsoids

Let us first derive the formulas corresponding to replacing the original variables x_i with the new variables Δx_i , i.e., the formulas that are obtained by substituting the expression $x_i = \tilde{x}_i + \Delta x_i$ into the objective function (21). After substitution,

$$f = f_0 + \sum_{i=1}^n f_i \cdot (\tilde{x}_i + \Delta x_i) + \sum_{i=1}^n \sum_{j=1}^n a_{i,j} \cdot (\tilde{x}_i + \Delta x_i) \cdot (\tilde{x}_j + \Delta x_j).$$

Opening parentheses,

$$\begin{aligned} f &= f_0 + \sum_{i=1}^n f_i \cdot \tilde{x}_i + \sum_{i=1}^n f_i \cdot \Delta x_i + \sum_{i=1}^n \sum_{j=1}^n a_{i,j} \cdot \tilde{x}_i \cdot \tilde{x}_j + \\ &\quad \sum_{i=1}^n \sum_{j=1}^n a_{i,j} \cdot \tilde{x}_i \cdot \Delta x_j + \sum_{i=1}^n \sum_{j=1}^n a_{i,j} \cdot \Delta x_i \cdot \tilde{x}_j + \sum_{i=1}^n \sum_{j=1}^n a_{i,j} \cdot \Delta x_i \cdot \Delta x_j. \end{aligned}$$

Grouping together terms that do not contain Δx_i at all, terms that are linear in Δx_i , and terms that are quadratic in Δx_i , we get the desired formulas (24)–(26).

Let us now derive the formulas (29)–(32). By definition,

$$\Delta x_i = \Delta \mathbf{x} \cdot \mathbf{e}^{(i)}. \quad (\text{A6})$$

We want to represent Δx_i in terms of the values $y^k = \Delta \mathbf{x} \cdot \mathbf{v}^{(k)}$. To do that, we expand the vector $\mathbf{e}^{(i)}$ into the base $\mathbf{v}^{(1)}, \dots, \mathbf{v}^{(n)}$ to get

$$\mathbf{e}^{(i)} = \sum_{k=1}^n (\mathbf{e}^{(i)} \cdot \mathbf{v}^{(k)}) \cdot \mathbf{v}^{(k)}. \quad (\text{A7})$$

We know the coordinates $\mathbf{v}_i^{(k)}$ of each eigenvector $\mathbf{v}^{(k)}$ in the standard basis $\mathbf{e}^{(i)}$, so we can explicitly compute $\mathbf{e}^{(i)} \cdot \mathbf{v}^{(k)}$ as $\mathbf{v}_i^{(k)}$. Thus, (A7) turns into

$$\mathbf{e}^{(i)} = \sum_{k=1}^n v_i^{(k)} \cdot \mathbf{v}^{(k)}. \quad (\text{A8})$$

Using scalar product to multiply both sides of (A8) by $\Delta \mathbf{x}$,

$$\mathbf{e}^{(i)} \cdot \Delta \mathbf{x} = \sum_{k=1}^n v_i^{(k)} \cdot (\mathbf{v}^{(k)} \cdot \Delta \mathbf{x}). \quad (\text{A9})$$

Because $\mathbf{e}^{(i)} \cdot \Delta \mathbf{x} = \Delta x_i$ and $\mathbf{v}^{(k)} \cdot \Delta \mathbf{x} = y_k$, (A9) becomes

$$\Delta x_i = \sum_{k=1}^n v_i^{(k)} \cdot y_k,$$

which is exactly the desired formula (29). Substituting expression (29) into the formula (24), we see that

$$f(x_1, \dots, x_n) = f'_0 + \sum_{i=1}^n \sum_{k=1}^n f'_i \cdot v_i^{(k)} \cdot y_k + \sum_{i=1}^n \sum_{j=1}^n \sum_{k=1}^n \sum_{l=1}^n f_{i,j} \cdot v_i^{(k)} \cdot v_i^{(l)} \cdot y_k \cdot y_l,$$

which is the same as

$$\begin{aligned} f(x_1, \dots, x_n) &= \\ f'_0 + \sum_{k=1}^n &\left(\sum_{i=1}^n f'_i \cdot v_i^{(k)} \right) \cdot y_k + \sum_{k=1}^n \sum_{l=1}^n \left(\sum_{i=1}^n \sum_{j=1}^n f_{i,j} \cdot v_i^{(k)} \cdot v_i^{(l)} \right) \cdot y_k \cdot y_l, \end{aligned}$$

which is exactly the desired formulas (30)–(32).

Let us now derive the formulas (37)–(39). Formula (36) implies that $t_p = u^{(p)} \cdot y$. As in the derivation of formula (29) above, we see that

$$y_k = \sum_{p=1}^n u_k^{(p)} \cdot t_p.$$

As when we first used eigenvectors, substituting this expression into the formula (30) for the objective function, we find that the quadratic part turns into $\sum \mu_p \cdot t_p^2$, and that the linear part turns into

$$\sum_{k=1}^n g_k \cdot \left(\sum_{p=1}^n u_k^{(p)} \cdot t_p \right) = \sum_{p=1}^n \left(\sum_{k=1}^n u_k^{(p)} \cdot g_k \right) \cdot t_p,$$

i.e., exactly the formulas (38)–(39).

To complete the derivation, we must show that (33) indeed turns into (37). The values y_k are coordinates of the vector y with respect to the standard orthonormal basis $(1, 0, \dots, 0), \dots, (0, \dots, 0, 1)$. The sum $\sum y_k^2$ is thus the square of the length of this vector. The values t_p are coordinates of the same vector y with respect to another orthonormal basis, namely, the basis formed by the eigenvectors $u^{(1)}, \dots, u^{(n)}$. The sum $\sum t_p^2$ is thus also equal to the square of the length of this vector.

Thus, the sums $\sum y_k^2$ and $\sum t_p^2$ are always equal, and hence the condition (33) is indeed equivalent to the condition (37).

Glossary

affine transformation A geometric transformation in Euclidean space which maps parallel lines to parallel lines.

basis A set of vectors $\{a_0, a_1, \dots, a_n\}$ is a basis for a vector space if the vectors are linearly independent of each other and each vector in the vector space can be written uniquely as a linear combination of the basis vectors.

bisection method A recursive algorithm for finding a root to a function $f(x)$ equation on the interval $a \leq x \leq b$. The algorithm evaluates the function at the midpoint of the interval and tests whether the root occurs in the intervals $[a, (a + b)/2]$ and $[(a + b)/2, b]$ until $f((a + b)/2) \leq \epsilon$.

Cauchy distribution A probability distribution function having density $f(x) = \frac{1}{\pi} \frac{1}{1+x^2}$ over the interval $-\infty < x < +\infty$. This distribution has such heavy tails that its mean is not finite.

Dempster-Shafer structure In this report, a finite collection of intervals from the real line, each of which is associated with a non-negative value m , such that the sum of all such m 's is unity. The multivariate generalization of a Dempster-Shafer structure may have either multidimensional rectangular boxes or ellipsoids instead of intervals.

diagonalization The process of transforming a square matrix into an equivalent matrix with nonzero elements only on its diagonal.

eigenvalue and eigenvector A nonzero vector \mathbf{e} is an eigenvector of a square matrix \mathbf{A} if there exists a scalar λ (eigenvalue) such that $\mathbf{A}\mathbf{e} = \lambda\mathbf{e}$.

ellipse A geometric shape which has two focal elements x_1 and x_2 and two radii r_1 and r_2 such that $2A = r_1 + r_2$, where A is a constant.

ellipsoid A multivariate generalization of an ellipse.

focal element A component of a Dempster-Shafer structure for which the associated non-negative value m is larger than zero. In this report, a focal element will be an interval of the real line, or, in the multivariate case, a rectangular box or an ellipsoid.

Gram-Schmidt orthogonalization process is an algorithm to transform a non-orthogonal basis $\{w_1, \dots, w_n\}$ to an orthonormal basis $\{v_1, \dots, v_n\}$:

$$\mathbf{v}_k = \mathbf{w}_k - \sum_{j=1}^{n-1} \frac{\langle \mathbf{w}_k, \mathbf{v}_j \rangle}{\|\mathbf{v}_j\|^2} \mathbf{v}_j \text{ for } 2 \leq k \leq n,$$

where $\|\mathbf{v}_k\|$ denotes the length of the vector and $\langle \mathbf{w}_k, \mathbf{v}_j \rangle$ denotes the inner product between two vectors.

homogeneous A function is homogeneous of order a if $f(tx, ty) = t^a + f(x, y)$ where t is a scalar.

hyperplane A multivariate generalization of a plane.

indefinite matrix A symmetric matrix having both positive and negative eigenvalues.

infimum Greatest lower bound.

interval A constraint on the value that a number x can take on the real line $\underline{X} \leq x \leq \bar{X}$, where \underline{X} and \bar{X} are known respectively as the infimum and supremum.

interval vector A generalization of the concept of an interval to vector spaces.

Lagrangian multipliers A method for constrained nonlinear optimization.

Minkowski sum The sum of two sets from A and B : $\{a+b : a \in A, b \in B\}$, where $A, B \subset V$, and V is a vector space.

NP-hard Computationally intractable in the sense that, as the order of the problem increases, the effort needed to obtain a solution increases exponentially as a function that is bounded by no polynomial. Also called NP-complete.

orthonormal basis A basis where each vector has a length 1 and are mutually perpendicular to each other.

positive definite matrix A symmetric matrix \mathbf{A} is positive definite if all of its eigenvalues are greater than zero.

positive semidefinite matrix A symmetric matrix \mathbf{A} is positive semidefinite if at least one eigenvalue of matrix is equal to zero and the others are positive.

quadratic form A homogeneous quadratic expression $\sum_{i=1}^{i \leq k} \sum_{j=1}^{j \leq k} a_{i,j} x_i x_j$ where $a_{i,j}$ is a constant and x_i, x_j are variables in the expression.

response surface The (usually) univariate output from a function with (usually) multiple input dimensions, considered as a surface over the space of inputs.

response surface model An approximation of a multivariate function.

supremum Least upper bound.

zone of possible vectors See *interval vector*.

References

- [1] G. Belfonte and B. Bona, “An improved parameter identification algorithm for signal with unknown-but-bounded errors”, *Proc. 7th IFAC Symposium on Identification and Parameter Estimation*, York, UK, 1985.
- [2] R. Belman, *Introduction to matrix analysis*, McGraw-Hill, New York, 1960.
- [3] F. L. Chernousko, *Estimation of the Phase Space of Dynamical Systems*, Nauka Publ., Moscow, 1988 (in Russian).
- [4] F. L. Chernousko, *State Estimation for Dynamical Systems*, CRC Press, Boca Raton, Florida, 1994.
- [5] A.P. Dempster, “Upper and lower probabilities induced by a multi-valued mapping”, *Annals of Mathematical Statistics*, 1967, Vol. 38, pp. 325–339.
- [6] S. Ferson, *RAMAS Risk Calc 4.0 Software: Risk Assessment with Uncertain Numbers*, Lewis Publishers, Boca Raton, Florida, 2002.
- [7] S. Ferson, V. Kreinovich, L. Ginzburg and D.S. Myers, *Constructing Probability Boxes and Dempster-Shafer Structures*, Sandia National Laboratories, SAND2002-4015 Technical Report, Albuquerque, New Mexico, 2003.
- [8] A. F. Filippov, “Ellipsoidal estimates for a solution of a system of differential equations”, *Interval Computations*, 1992, No. 2(4), pp. 6–17.
- [9] A. Finkelstein, O. Kosheleva, and V. Kreinovich, “Astrogeometry, error estimation, and other applications of set-valued analysis”, *ACM SIGNUM Newsletter*, 1996, Vol. 31, No. 4, pp. 3–25.
- [10] E. Fogel and Y. F. Huang, “One the value of information in system identification. Bounded noise case”, *Automatica*, 1982, Vol. 18, pp. 229–238.
- [11] C. F. Gerald and P. O. Wheatley, *Applied Numerical Methods*, Addison-Wesley, Reading, Massachusetts, 2004.
- [12] G. H. Golub and C. F. Van Loan, *Matrix Computations*, John Hopkins University Press, Baltimore, 1996.
- [13] W. Hastings. “Mone Carlo sampling methods using Markov chains and their applications”, *Biometrika*, 1970, Vol. 57, pp. 97–109.
- [14] L. W. Jackson. “A comparison of ellipsoidal and interval arithmetic error bounds”. *SIAM Review*, 1969, Vol. 11, p 114.

- [15] C. Joslyn. “Aggregation and completion of random sets with distributional fuzzy measures”. *Int. J. of Uncertainty, Fuzziness, and Knowledge-Based Systems*, 1996, Vol. 4, p 307-329.
- [16] W. M. Kahan. “Circumscribing an ellipsoid about the intersections of two ellipsoids. *Canadian Mathematical Bulletin*, 1968, Vol. 11, pp. 437–.
- [17] G. Klir and B. Yuan, *Fuzzy Sets and Fuzzy Logic: Theory and Applications*, Prentice Hall, Upper Saddle River, NJ, 1995.
- [18] V. Kreinovich, A. Lakeyev, J. Rohn, and P. Kahl, *Computational Complexity and Feasibility of Data Processing and Interval Computations*, Kluwer, Dordrecht, 1998.
- [19] S. Li, Y. Ogura, and V. Kreinovich, *Limit Theorems and Applications of Set Valued and Fuzzy Valued Random Variables*, Kluwer Academic Publishers, Dordrecht, 2002.
- [20] N. Metropolis, A. Rosenbluth, M. Rosenbluth, A. Teller and E. Teller. “Equations of state calculations by fast computing machines, 3”, *Chem. Phys.*, 1953, Vol. 21, pp. 1087–1092.
- [21] R.E. Moore. *Interval Analysis*. Prentice-Hall, Englewood Cliffs, NJ, New York, 1966.
- [22] A. Neumaier. *Interval Methods for System of equations*, Cambridge University Press, Cambridge, U.K, 1990.
- [23] A. Neumaier, “The wrapping effect, ellipsoid arithmetic, stability and confidence regions”, *Computing Supplementum* Vol. 9, 1993, pp. 175–190.
- [24] H. T. Nguyen and V. Kreinovich, “Nested Intervals and Sets: Concepts, Relations to Fuzzy Sets, and Applications”, In: R. B. Kearfott and Vladik Kreinovich, *Applications of Interval Computations*, Kluwer, Dordrecht, 1996, pp. 245–290
- [25] H. T. Nguyen and E. A. Walker, *First Course in Fuzzy Logic*, CRC Press, Boca Raton, Florida, 1999.
- [26] F. C. Scheppe, “Recursive state estimation: unknown but bounded errors and system inputs”, *IEEE Transactions on Automatic Control*, 1968, Vol. 13, p. 22.
- [27] F. C. Scheppe, *Uncertain Dynamics Systems*, Prentice Hall, Englewood Cliffs, New Jersey, 1973.
- [28] K. Sentz and S. Ferson, *Combination of Evidence in Dempster-Shafer Theory*, Sandia National Laboratories, SAND2002-0835 Technical Report, Albuquerque, New Mexico, 2002.

- [29] G. Shafer, *A Mathematical Theory of Evidence*, Princeton University Press, Princeton, New Jersey, 1976.
- [30] G. Shafer, “A mathematical theory of evidence”, *The AI Magazine*, 1984, pp. 81–83.
- [31] G. Shafer, “The combination of evidence”, *International Journal of Intelligent Systems*, 1986, Vol. 1, pp. 155–179.
- [32] S. T. Soltanov, “Asymptotic of the function of the outer estimation ellipsoid for a linear singularly perturbed controlled system”, In: S. P. Shary and S. P. Shokin (eds.), *Interval Analysis*, Krasnoyarsk, Academy of Sciences Computing Center, Publication No. 17, 1990, pp. 35–40 (in Russian).
- [33] R. Trejo and V. Kreinovich, “Error Estimations for Indirect Measurements: Randomized vs. Deterministic Algorithms For ‘Black-Box’ Programs”, In: S. Rajasekaran, P. Pardalos, J. Reif, and J. Rolim (eds.), *Handbook on Randomized Computing*, Kluwer, 2001, pp. 673–729.
- [34] G. S. Utyubaev, “On the ellipsoid method for a system of linear differential equations”, In: S. P. Shary (ed.), *Interval Analysis*, Krasnoyarsk, Academy of Sciences Computing Center, Publication No. 16, 1990, pp. 29–32 (in Russian).
- [35] S. A. Vavasis, *Nonlinear Optimization: Complexity Issues*, Oxford University Press, New York, 1991.
- [36] H. M. Wadsworth Jr., *Handbook of statistical methods for engineers and scientists*, McGraw-Hill, N.Y., 1990.
- [37] R.R. Yager, “Arithmetic and other operations on Dempster-Shafer structures”, *International Journal of Man-Machine Studies*, 1986, Vol. 25, pp. 357–366.

DISTRIBUTION

External Distribution

Prof. G. E. Apostolakis
Department of Nuclear Engineering
Massachusetts Institute of Technology
Cambridge, MA 02139-4307

Prof. Bilal Ayyub
University of Maryland
Center for Technology & Systems Management
Civil & Environmental Engineering
Rm. 0305 Martin Hall
College Park, MD 20742-3021

Prof. Ivo Babuska
TICAM
Mail Code C0200
University of Texas at Austin
Austin, TX 78712-1085

S. Balachandar
Dept. of Mechanical & Aerospace Engr.
University of Florida
231 MAE-A, PO Box 116250
Gainesville, FL 32611-6205

Osman Balci
Department of Computer Science
Virginia Tech
Blacksburg, VA 24061

Prof. Bruce Beck
University of Georgia
D.W. Brooks Drive
Athens, GA 30602-2152

Prof. James Berger
Inst. of Statistics and Decision Science
Duke University
Box 90251
Durham, NC 27708-0251

Prof. Daniel Berleant
Department of Information Science
University of Arkansas at Little Rock
ETAS Building, Room 258 D
2801 South University Avenue
Little Rock, Arkansas 72204

Prof. V. M. Bier
Department of Industrial Engineering
University of Wisconsin
Madison, WI 53706

Mark Brandyberry
Computational Science and Engineering
2264 Digital Computer Lab, MC-278
1304 West Springfield Ave.
University of Illinois .
Urbana, IL 61801

John A. Cafeo
General Motors R&D Center
Mail Code 480-106-256
30500 Mound Road
Box 9055
Warren, MI 48090-9055

Andrew Cary
The Boeing Company
MC S106-7126
P.O. Box 516
St. Louis, MO 63166-0516

James C. Cavendish
General Motors R&D Center
Mail Code 480-106-359
30500 Mound Road
Box 9055
Warren, MI 48090-9055

Chun-Hung Chen
Department of Systems Engineering &
Operations Research
George Mason University
4400 University Drive, MS 4A6
Fairfax, VA 22030

Wei Chen
Department of Mechanical Engineering
Northwestern University
2145 Sheridan Road, Tech B224
Evanston, IL 60208-3111

Kyeongjae Cho
Dept. of Mechanical Engineering
MC 4040
Stanford University
Stanford, CA 94305-4040

Hugh Coleman
Department of Mechanical &
Aero. Engineering
University of Alabama/Huntsville
Huntsville, AL 35899

Roger Cooke
Resources for the Future
1616 P Street NW
Washington, DC 20036

Prof. Allin Cornell
Department of Civil and Environmental
Engineering
Terman Engineering Center
Stanford University
Stanford, CA 94305-4020

Raymond Cosner (2)
Boeing-Phantom Works
MC S106-7126
P. O. Box 516
St. Louis, MO 63166-0516

Thomas A. Cruse
AFRL Chief Technologist
1981 Monahan Way
Bldg. 12, Room 107
Wright-Patterson AFB, OH 45433-7132

Prof. Alison Cullen
University of Washington
Box 353055
208 Parrington Hall
Seattle, WA 98195-3055

Prof. U. M. Diwekar
Center for Uncertain Systems, Tools for
Optimization, and Management
Vishwamitra Research Institute
34 N. Cass Avenue
Westmont, IL 60559

Prof. David Draper
Applied Math & Statistics
147 J. Baskin Engineering Bldg.
University of California
1156 High St.
Santa Cruz, CA 95064

Isaac Elishakoff
Dept. of Mechanical Engineering
Florida Atlantic University
777 Glades Road
Boca Raton, FL 33431-0991

Ashley Emery
Dept. of Mechanical Engineering
Box 352600
University of Washington
Seattle, WA 98195-2600

Prof. Donald Estep
Department of Mathematics
Colorado State University
Fort Collins, CO 80523

Scott Ferson
Applied Biomathematics
100 North Country Road
Setauket, New York 11733-1345

Prof. C. Frey
Department of Civil Engineering
Box 7908, NCSU
Raleigh, NC 27659-7908

Prof. Roger Ghanem
254C Kaprielian Hall
Dept. of Civil Engineering
3620 S. Vermont Ave.
University of Southern California
Los Angles, CA 90089-2531

Prof. James Glimm
Dept. of Applied Math & Statistics
P138A
State University of New York
Stony Brook, NY 11794-3600

Prof. Ramana Grandhi
Dept. of Mechanical and Materials
Engineering
3640 Colonel Glenn Hwy.
Dayton, OH 45435-0001

Prof. Raphael Haftka
Dept. of Aerospace and Mechanical
Engineering and Engineering Science
P.O. Box 116250
University of Florida
Gainesville, FL 32611-6250

Prof. Yacov Y. Haimes
Center for Risk Management of Engineering
Systems
D111 Thornton Hall
University of Virginia
Charlottesville, VA 22901

Achintya Haldar
Dept. of Civil Engineering
& Engineering Mechanics
University of Arizona
Tucson, AZ 85721

Tim Hasselman
ACTA
2790 Skypark Dr., Suite 310
Torrance, CA 90505-5345

Prof. Steve Hora
Institute of Business and Economic Studies
University of Hawaii, Hilo
523 W. Lanikaula
Hilo, HI 96720-4091

R.L. Iman
Southwest Technology Consultants
1065 Tramway Lane, NE
Albuquerque, NM 87122

George Karniadakis
Division of Applied Mathematics
Brown University
192 George St., Box F
Providence, RI 02912

Prof. George Klir
Binghamton University
Thomas J. Watson School of Engineering &
Applied Sciences
Engineering Building, T-8
Binghamton NY 13902-6000

Vladik Kreinovich
Department of Computer Science
University of Texas at El Paso
500 W. University
El Paso, TX 79968, USA

Averill M. Law
6601 E. Grant Rd.
Suite 110
Tucson, AZ 85715

Prof. Sankaran Mahadevan
Vanderbilt University
Dept. of Civil and Environmental Engineering
Box 6077, Station B
Nashville, TN 37235

Prof. Max Morris
Department of Statistics
Iowa State University
304A Snedecor-Hall
Ames, IA 50011-1210

Prof. Ali Mosleh
Center for Reliability Engineering
University of Maryland
College Park, MD 20714-2115

Zissimos P. Mourelatos
Dept. of Mechanical Engineering
School of Engr. and Computer Science
Rochester, MI 48309-4478

Rafi Muhanna
Regional Engineering Program
Georgia Tech
210 Technology Circle
Savannah, GA 31407-3039

NASA/Ames Research Center (2)
Attn: Unmeel Mehta, MS 229-3
David Thompson, MS 269-1
Moffett Field, CA 94035-1000

NASA/Glenn Research Center (2)
Attn: John Slater, MS 86-7
Chris Steffen, MS 5-11
21000 Brookpark Road
Cleveland, OH 44135

NASA/Langley Research Center (7)
Attn: Dick DeLoach, MS 236
Michael Hemsch, MS 499
Jim Luckring, MS 286
Joe Morrison, MS 128
Ahmed Noor, MS 369
Sharon Padula, MS 159
Thomas Zang, MS 449
Hampton, VA 23681-0001

Prof. Efstratios Nikolaidis
MIME Dept.
4035 Nitschke Hall
University of Toledo
Toledo, OH 43606-3390

William L. Oberkampf
2014 Monte Largo Dr. NE
Albuquerque, NM 87112

Tinsley Oden
TICAM
Mail Code C0200
University of Texas at Austin
Austin, TX 78712-1085

Prof. M. Elisabeth Paté-Cornell
Department of Industrial Engineering and
Management
Stanford University
Stanford, CA 94305

Prof. Adrian E. Raftery
Department of Statistics
University of Washington
Seattle, WA 98195

Ramesh Rebba
General Motors R&D Center
Mail Code 480-106-256
30500 Mound Road
Box 9055
Warren, MI 48090-9055

Prof. John Renaud
Dept. of Aerospace & Mechanical Engr.
University of Notre Dame
Notre Dame, IN 46556

Patrick J. Roache
1215 Apache Drive
Socorro, NM 87801

Prof. Tim Ross
Dept. of Civil Engineering
University of New Mexico
Albuquerque, NM 87131

Chris Roy
Aerospace and Ocean Engineering Dept.
215 Randolph Hall
Virginia Tech
Blacksburg, VA 24061-0203

Prof. J. Sacks
Inst. of Statistics and Decision Science
Duke University
Box 90251
Durham, NC 27708-0251

Len Schwer
Schwer Engineering & Consulting
6122 Aaron Court
Windsor, CA 95492

Prof. Nozer D. Singpurwalla
The George Washington University
Department of Statistics
2140 Pennsylvania Ave. NW
Washington, DC 20052

Prof. C.B. Storlie
Department of Mathematics and Statistics
University of New Mexico
Albuquerque, NM 87131-0001

Southwest Research Institute (3)
Attn: B. Bichon
J. McFarland
B. Thacker
P.O. Drawer 28510
622 Culebra Road
San Antonio, TX 78284

Raul Tempone
School of Computational Science
400 Dirac Science Library
Florida State University
Tallahassee, FL 32306-4120

Prof. Fulvio Tonon
Department of Civil Engineering
University of Texas at Austin
1 University Station C1792
Austin, TX 78712-0280

Robert W. Walters
Aerospace and Ocean Engineering
Virginia Tech
215 Randolph Hall, MS 203
Blacksburg, VA 24061-0203

Prof. Karen E. Willcox
Department of Aeronautics & Astronautics
Massachusetts Institute of Technology
77 Massachusetts Ave
Room 37-447
Cambridge, MA 02139

Byeng D. Youn
Department of Mechanical Engineering
0158 Glenn Martin Hall
University of Maryland
College Park, Maryland 20742

Foreign Distribution

Michael Beer
Dept. of Civil Engineering
National University of Singapore
BLK E1A, #07-03, 1 Engineering Drive 2
SINGAPORE 117576

Prof. Yakov Ben-Haim
Department of Mechanical Engineering
Technion-Israel Institute of Technology
Haifa 32000
ISRAEL

Prof. A.P. Bourgeat
UMR 5208 – UCB Lyon1, MCS, Bât. ISTIL
Domaine de la Doua; 15 Bd. Latarjet
69622 Villeurbanne Cedex
FRANCE

CEA Cadarache (2)
Attn: Nicolas Devictor
Bertrand Iooss
DEN/CAD/DER/SESI/CFR
Bat 212
13108 Saint Paul lez Durance cedex
FRANCE

Etienne de Rocquigny
EDF R&D MRI/T56
6 quai Watier
78401 Chatou Cedex
FRANCE

European Commission (5)
Attn: Francesca Campolongo
Mauro Ciechetti
Marco Ratto
Andrea Saltelli
Stefano Tarantola
JRC Ispra, ISIS
2 1020 Ispra
ITALY

Régis Farret
Direction des Risques Accidentels
INERIS
BP2 – 60550 Verneuil en Halatte
FRANCE

Prof. Jim Hall
University of Bristol
Department of Civil Engineering
Queens Building, University Walk
Bristol UK 8581TR

Prof. J.P.C. Kleijnen
Department of Information Systems
Tilburg University
5000 LE Tilburg
THE NETHERLANDS

Philipp Limbourg
University of Duisburg-Essen,
Bismarckstr. 90, 47057
Duisburg
GERMANY

Prof. A. O'Hagan
Department of Probability and Statistics
University of Sheffield
Hicks Building
Sheffield S3 7RH
UNITED KINGDOM

Prof. G.I. Schüller
Institute of Engineering Mechanics
Leopold-Franzens University
Technikerstrasse 13
6020 Innsbruck
AUSTRIA

Prof. H.P. Wynn
Department of Statistics
London School of Economics
Houghton Street
London WC2A 2AE
UNITED KINGDOM

Department of Energy Laboratories

Department of Energy (3)
Forrestal Building
1000 Independence Ave., SW
Washington, DC 20585
Attn: Njema Frazier, NA-114
Bob Meisner, NA-114
K. Pao, NA-114

Idaho National Laboratory (2)
2525 Fremont Ave.
P.O. Box 1625
Idaho Falls, ID 83415
Attn: Dana A. Knoll, MS 3855
Richard R. Schultz, MS 3890

Lawrence Livermore National Laboratory (6)							
7000 East Ave.	1	MS 0376	1421	T. D. Blacker			
P.O. Box 808	1	MS 1319	1422	J. A. Ang			
Livermore, CA 94550	1	MS 0822	1424	D. Rogers			
Attn: Frank Graziani	1	MS 0378	1431	R. M. Summers			
Richard Klein	1	MS 0370	1433	J. Strickland			
J. F. McEnerney	1	MS 0370	1433	G. Backus			
Joe Sefcik	1	MS 0370	1433	M. Boslough			
Charles Tong	1	MS 0370	1433	D. Schoenwald			
Los Alamos National Laboratory (8)							
Mail Station 5000	1	MS 1322	1435	J. B. Aidun			
P.O. Box 1663	1	MS 0316	1437	J. Castro			
Los Alamos, NM 87545	1	MS 0316	1437	J. N. Shadid			
Attn: Mark C. Anderson, MS T080	1	MS 0384	1500	A.C. Ratzel			
Jerry S. Brock, MS F663	1	MS 0824	1500	T.Y. Chu			
Scott Doebling, MS T080	1	MS 0836	1500	M.R. Baer			
Francois Hemez, MS F699	1	MS 0346	1514	D. Dobranich			
David Higdon, MS F600	1	MS 0836	1514	R. E. Hogan			
James Kamm, MS D413	1	MS 0825	1515	D. W. Kuntz			
Kari Sentz, MS F600	1	MS 0825	1515	J. L. Payne			
Brian Williams, MS F600	1	MS 0836	1516	W. P. Wolfe			
	1	MS 0372	1520	J. S. Lash			
Pacific Northwest National Laboratory (2)							
Risk and Decision Science Group	1	MS 0847	1520	J.M. Redmond			
Richland, WA 99352-2458	1	MS 0557	1522	P. J. Wilson			
Attn: Stephen D. Unwin	1	MS 0346	1523	C. C. O'Gorman			
	1	MS 0557	1523	T. J. Baca			
	1	MS 0372	1523	T. Simmermacher			
	1	MS 0372	1524	J. Pott			
	1	MS 0372	1524	T. D. Hinnerichs			
Sandia Internal Distribution							
	1	MS 0372	1524	K. E. Metzinger			
	1	MS 1070	1526	C. C. Wong			
	1	MS 0821	1530	A.L. Thornton			
	1	MS 1135	1532	S.R. Tieszen			
	1	MS 1135	1532	T. K. Blanchat			
	1	MS 0847	1535	J.L. Cherry			
	1	MS 0833	1536	R. O. Griffith			
	1	MS 1318	1540	D. E. Womble			
	1	MS 0382	1541	B. Hassan			
	1	MS 0382	1541	H. C. Edwards			
	1	MS 0380	1541	G. D. Sjaardema			
	1	MS 0380	1542	J. Jung			
	1	MS 0380	1542	M. W. Heinstein			
	1	MS 0380	1542	G. M. Reese			
	1	MS 0828	1544	A. A. Giunta			
	1	MS 0828	1544	A. R. Black			
	1	MS 0382	1544	K. D. Copps			
Waanders							
	1	MS 0828	1544	K. J. Dowding			
	1	MS 1318	1414	A. G. Salinger			
	1	MS 1318	1415	S. K. Rountree			
	1	MS 1318	1415	D. Dunlavy			
	1	MS 1320	1416	S. S. Collis			
	1	MS 1316	1416	S. J. Plimpton			
	1	MS 1320	1416	M. Heroux			
	1	MS 1322	1420	S. S. Dosanjh			
	1	MS 1322	1420	J. Tompkins			
	1	MS 0557	1544	T. L. Paez			
	1	MS 0828	1544	J. R. Red-Horse			
	1	MS 0828	1544	V. J. Romero			
	1	MS 0847	1544	W. R. Witkowski			
	1	MS 0382	1545	E. S. Hertel			
	1	MS 0384	1550	P. Yarrington			

1	MS 0828	1551	M. Pilch
1	MS 0457	2011	R. A. Paulsen
1	MS 0479	2134	S. E. Klenke
1	MS 0447	2111	J. F. Lorio
1	MS 0521	2617	E. A. Boucheron
1	MS 0453	2900	L. S. Walker
1	MS 0374	2991	H. P. Walther
1	MS 1231	5223	S. N. Kempka
1	MS 0529	5350	K. D. Meeks
1	MS 1153	5441	L. C. Sanchez
1	MS 0831	5500	M. O. Vahle
1	MS 0972	5572	S. E. Lott
1	MS 1373	6721	S. M. DeLand
1	MS 1138	6322	P. G. Kaplan
1	MS 1137	6323	G. D. Valdez
1	MS 1124	6333	P. S. Veers
1	MS 0757	6414	G. D. Wyss
1	MS 1002	6470	P. D. Heermann
1	MS 0748	6761	D. G. Robinson
1	MS 0778	6780	P. N. Swift
1	MS 0776	6781	R. P. Rechard
1	MS 0776	6782	R. J. MacKinnon
1	MS 0778	6782	B. W. Arnold
1	MS 0776	6784	C. M. Sallaberry
1	MS 0776	6786	J. S. Stein
1	MS 1399	6787	P. Vaughn
1	MS 9404	8240	E. P. Chen
1	MS 9042	8246	M. L. Chiesa
1	MS 9042	8249	J. J. Dike
1	MS 9404	8246	J. A. Zimmerman
1	MS 9151	8900	L. M. Napolitano
1	MS 9159	8962	H. R. Ammerlahn
1	MS 9159	8962	P. D. Hough
1	MS 9152	8964	M. F. Hardwick
1	MS 0428	12300	L. A. Schoof
1	MS 0428	12330	T. R. Jones
1	MS 0830	12335	K. V. Diegert
1	MS 0829	12337	J. M. Sjulin
1	MS 0829	12337	B. M. Rutherford
1	MS 0638	12341	D. E. Peercy
1	MS 0405	12346	R. Kreutzfeld
1	MS 0492	12332	T. D. Brown
1	MS 0405	12347	R. D. Waters
1	MS 1030	12870	J. G. Miller
1	MS 0899	9536	Technical Library (electronic copy)